

~~RESTRICTED~~ UNCLASSIFIED *4x Dryden per race* *7/3/63*
release classed DOCUMENT

NACA for 419
Dir. Assoc. Research
NACA

By *m H H*
1-23-51
See *22*

NACA

This document contains classified information affecting the National Defense of the United States within the meaning of the Espionage Act. Its transmission or the revelation of its contents in any manner to an unauthorized person is prohibited by law.

Information so classified may be supplied only to persons in the military and naval services of the United States, agents and employees of the Government, and employees of the contractors who have access to such information, and to persons who of necessity must be informed thereof.

RESEARCH MEMORANDUM

for the

Bureau of Aeronautics, Navy Department

WIND-TUNNEL TESTS TO DETERMINE AILERON
CHARACTERISTICS OF THE MCDONNELL XF-1 AIRPLANE

TEST NO. NACA 23102

By

Campbell C. Yates and Leslie E. Schnitzer

Langley Memorial Aeronautical Laboratory
Langley Field, Va.

~~RESTRICTED PROPRIETARY INFORMATION~~

Sept. 26, 1946

NATIONAL ADVISORY COMMITTEE FOR AERONAUTICS

WASHINGTON

NATIONAL ADVISORY COMMITTEE FOR AERONAUTICS

RESEARCH MEMORANDUM

WIND-TUNNEL TESTS TO DETERMINE AILERON
CHARACTERISTICS OF THE MCDONNELL XFD-1 AIRPLANE

TED NO. NACA 23102

By Campbell C. Yates and Leslie E. Schreiber

SUMMARY

Tests were performed on a partial span of the wing of a McDonnell XFD-1 airplane to determine a combination of sealed internal balance and spring-tab stiffness for the aileron that would give satisfactory stick-force characteristics for the airplane. Two sealed internal balances were tested in combination with spring tabs of various stiffnesses. One of the combinations was tested at several speeds to determine the variation of stick force with speed.

Estimates, based on the results of the tests, indicate that for this airplane any reduction of stick force by use of the spring tab reduces the helix angle $pb/2V$ below the required value of 0.09. The estimates show that, of the configurations tested, the most satisfactory combination for obtaining a stick force of 30 pounds at 300 miles per hour indicated airspeed is a 0.48-chord internal balance in combination with a spring-tab stiffness of 500 pounds per inch. With this combination, a wing-tip helix angle of 0.078 is estimated. Stick-force curves for all configurations show a rapid increase in stick force above approximately 20° total aileron deflection.

Estimates were also made of the stick force for the 0.48-chord internal balance in combination with a spring-tab stiffness of 1000 pounds per inch, assuming the existing linear aileron-stick linkage replaced by a nonlinear aileron-stick linkage. The estimate shows that a nearly linear stick-force gradient with aileron deflection is obtained with a maximum stick force of 30 pounds and a $pb/2V$ of 0.083 at full deflection of 30° . Further modification of the aileron system to permit approximately 33° total aileron deflection would give the required wing-tip helix angle of 0.09 at a stick force of about 33 pounds.

INTRODUCTION

At the request of the Bureau of Aeronautics, Navy Department, a portion of the outer panel of a McDonnell XFD-1 airplane wing was tested in the Langley high-speed 7- by 10-foot tunnel. The purpose of the tests was the determination of an aileron balance spring-tab configuration which would give satisfactory stick-force characteristics.

The aileron balance arrangement on the XFD-1 airplane is an internally sealed balance in combination with a spring tab. Two internal-balance arrangements were tested with springs of various stiffnesses in the spring-tab system to determine a combination or combinations which would meet the stated requirements.

SYMBOLS

The coefficients and symbols used in the presentation of the results are:

C_L	lift coefficient (L/qS)
C_l	rolling-moment coefficient (L^*/qSb)
C_{h_a}	aileron hinge-moment coefficient ($H_a/qb_a\bar{c}_a^2$), positive when moment tends to depress trailing edge of aileron
ΔP	seal-pressure coefficient, pressure below seal minus pressure above seal divided by the free-stream dynamic pressure
C_{l_p}	rate of change of rolling-moment coefficient C_l , with helix angle ($pb/2V$)
L	lift of the semispan portion of wing tested, pounds
L^*	rolling moment about plane of symmetry of airplane caused by deflection of one aileron on a complete wing of airplane plan form, foot-pounds
H_a	aileron hinge moment, foot-pounds
q	free-stream dynamic pressure, pounds per square foot ($\rho V^2/2$)
S	area of airplane wing, square feet
b	span of airplane wing, feet

b_a	span of aileron along hinge line, feet
\overline{c}_a	root-mean-square chord of aileron behind hinge axis, feet
$pb/2V$	helix angle described by tip of wing in roll, radians
p	rolling velocity, radians per second
V	free-stream velocity, feet per second
ρ	density of air, slugs per cubic foot
α	angle of attack of root of airplane wing
δ_a	aileron deflection, degrees; positive when trailing edge of aileron is below chord plane of wing
δ_{st}	spring-tab deflection, degrees; measured with respect to aileron chord plane, positive when trailing edge of tab is below chord plane of aileron
δ_s	stick deflection, degrees
M	Mach number
c	local wing chord
c_a	local aileron chord behind hinge axis
c_b	local balance chord, measured between hinge axis and center of overhang gap
a_o	section lift-curve slope per degree for incompressible flow

MODEL AND APPARATUS

Model

A portion of the outer panel of an XFD-1 airplane wing was supplied by the McDonnell company for these tests. The important geometric characteristics of the panel tested and the complete airplane wing are presented in table I and a detailed sketch of the panel tested is given in figure 1. The general arrangement of the airplane, showing the portion of the actual wing used for these tests, is presented in figure 2.

Sketches of an inboard and an outboard section of the 44-percent and 48-percent balances are shown in figures 3 and 4, respectively. The seal was divided into two chambers by the center aileron hinge. Vinylite-coated nylon fabric was used to seal the nose plates of the internal balance to the front and sides of the balance chamber. The seal extended aft to approximately the hinge center line at the inboard and outboard ends of the aileron, and was arranged at the center hinge so that the seal was complete across the hinge. Pressure differences across the seal were measured by means of tubes installed in the balance chambers at the locations shown in figure 1.

The wing panel, as supplied, had the leading edge of the aileron covered with a doped fabric to seal some access holes in the metal skin. During the tests, this fabric pulled off and was replaced with a 1/32-inch-thick aluminum plate fixed to the leading edge with sheet-metal screws, gummed fabric tape being placed between the aileron skin and the plates as a seal. The rear edge of the plate was beveled to fair smoothly into the surface of the aileron. Check tests showed no appreciable effect of the metal plate on the aileron hinge moments.

A sketch of the spring-tab mechanism is shown in figure 5. Springs having moduli of 28 and 500 pounds per inch were supplied by the McDonnell company, and were calibrated at Langley. A 1500-pound-per-inch spring was made and calibrated at Langley. The spring tab, as shown in figure 5, was mounted on the aileron by means of a piano hinge and was otherwise unsealed. The tab had no aerodynamic balance.

Test Installation

The model was mounted horizontally on the side model support of the balance frame of the Langley high-speed 7- by 10-foot tunnel as shown in figures 6(a) and 6(b). The root chord of the model was adjacent to the tunnel wall, the tunnel wall thereby serving as a reflection plane. Although a small clearance was maintained between the model and the tunnel wall, no part of the model was attached to, or came in contact with the tunnel wall. A flange at the root of the wing served as a shield to deflect the air flow through the hole in the tunnel wall so as to minimize the effects of this inflow on the flow over the model.

The angle of attack of the wing panel was set according to a quadrant painted on the tunnel wall at the trailing edge of the wing as shown in figure 6(a). The aileron angle was adjusted from outside the tunnel by means of a lead screw inside the wing. An

electric strain gage was mounted on one arm of the bell crank to facilitate measurement of the aileron hinge moments. The wing panel as supplied had remote indicating electric position indicators for both the tab and aileron. Vibration of the model damaged the gears in the indicators and midway in the test program they were replaced with the quadrants which can be seen in figure 6(a).

Corrections

The dynamic pressures and Mach numbers have been corrected for the constriction effects of the model in the tunnel by the methods given in reference 1. The angles of attack and moment coefficients have been corrected for the effect of the tunnel jet boundaries by the general methods given in reference 2. Additional corrections were applied to convert the rolling-moment data for the test wing plan form to that for the complete airplane wing plan form. Plan-form corrections were not applied to the hinge moments or the pressure coefficients, since the magnitude of these corrections was not known.

The combined jet-boundary and plan-form corrections applied are as follows:

$$C_L = 0.971C_{L_u}$$

$$\alpha = \alpha_u + 0.578C_L$$

$$C_l = 0.448C_{l_u}$$

$$C_{ha} = C_{ha_u} + \frac{K}{1 - M^2} C_{L_u}$$

C_b/C_a	K
0.44	0.0192
.48	.0159

where the subscript u denotes uncorrected coefficients.

The pressure coefficients were not corrected for jet-boundary effects.

TESTS

The majority of the tests were run at a dynamic pressure of 229 pounds per square foot. Several tests were also performed at dynamic pressures of 459 and 31 pounds per square foot. The corresponding indicated airspeeds, Mach numbers and Reynolds numbers were as follows:

q (lb/sq ft)	Tunnel airspeed (mph)	Mach number	Reynolds number (based on M.A.C. of test panel)
31	112	0.146	5.3×10^6
229	313	.416	13.9
459	459	.630	18.3

In an effort to expedite the testing, the angle of attack of the wing of the airplane in roll for a given aileron deflection was estimated for the fully loaded airplane at 300 miles per hour indicated airspeed. To allow for errors in the estimation of rate of roll of the airplane, an envelope of angle of attack covering a range roughly plus and minus 1° from the angle calculated for each aileron deflection was set up for most tests.

A number of tests were run using only the estimated angle of attack as sufficiently accurate estimates of stick force could be made from the data to show the stick force characteristics expected for that configuration. For the case in which the spring tab was operating, mechanical interference resulted in inconsistent hinge-moment data for aileron angles greater than 12° and -14° . These tests were therefore limited to that deflection range.

A total of about 35° spring-tab deflection was available. For the majority of the tests, this total was equally divided between up and down deflection, but for several of the tests, the spring tab was set with about -3° deflection to give slightly more negative than positive tab deflection.

The trim tab was fixed at neutral for all the tests.

The $0.44 \frac{c_b}{c_a}$ balance was tested with the spring tab blocked at $\delta_{st} = 0^\circ$ and with the spring tab equipped with springs having moduli of 28, 500 pounds per inch, and the $0.48 \frac{c_b}{c_a}$ balance with the spring tab blocked at $\delta_{st} = 0^\circ$ and with springs having moduli of 28, 500, and 1500 pounds per inch.

Before the force tests were started, an attempt was made to check the amount of leakage in the sealed internal balance. A sketch of the seal-leakage test setup is shown in figure 7. In these tests the pressure box shown on the figure was mounted on the upper surface of the wing over the vent gap in such a manner as to open into both the inboard and outboard upper seal chamber. All openings from the upper seal chamber, through the upper vent gap to the atmosphere were sealed with cellulose tape. Only that part of the vent gap opening into the pressure box was left open. A low-pressure source was connected to one end of the pressure box. The pressure tubes in the seal chamber and tubes leading into the pressure box were coupled to manometers to determine the pressures in the seal chambers and pressure box. The seal leakage factor E is defined as:

$$E = 1 - \frac{P_a - P_b}{P_c - P_d}$$

where

$P_a - P_b$ pressure difference across seal

$P_c - P_d$ pressure difference between pressure box and atmosphere
(pressure difference across vents)

During the course of the tests, the leading edge of the model became roughened by the impact of particles of dust in the tunnel air stream. The resulting rough leading edge probably fixed transition at the leading edge of the airfoil. The nicks in the leading edge were not filled during the tests, however, as it was believed that the leading edge of the wing on a service airplane would probably become similarly damaged under normal flight conditions and that the condition of the model would be somewhat similar to the condition of the normal airplane.

RESULTS AND DISCUSSION

Data. - Seal-pressure coefficient data for the various configurations are presented in figures 8 and 9. The rolling-moment and hinge-moment coefficients for the configurations tested are shown in figures 10 and 11. Figures 12 and 13 present stick forces and rates of roll for different configurations and airspeeds. Estimated stick forces for the 0.48 c_b/c_a internal balance with a

1000-pound-per-inch spring-tab stiffness and a nonlinear aileron-stick linkage are shown in figure 14. This linkage arrangement and the variation of the mechanical advantage are also shown in figure 14. A comparison of estimated aileron characteristics with those obtained in flight is shown in figure 15. Figures 16 and 17 present the spring-tab characteristics.

Seal pressures.- Comparison of the seal-pressure coefficient data (figs. 8 and 9) with data from tests of wind-tunnel models having a small percentage of leakage (reference 3) shows the pressure coefficients for this model are low. It is believed that the low pressure coefficients are the result of leakage around the hinges and the seal as well as the fact that the cover plates were not true contour. Leakage tests of the $0.44 \frac{c_b}{c_a}$ balance gave a value of E of approximately 0.10. This amount of leakage probably caused most of the loss in pressure coefficient resulting from aileron deflection.

Stick forces.- The method of calculation of the stick forces is described in the appendix.

It will be noted from figures 12 and 13 that there is a rapid increase in stick force past approximately 20° total aileron deflection. This rise in stick force is the result of the rapid increase in hinge moment for the upgoing aileron caused by a decrease in $\frac{\partial \Delta P}{\partial \delta_a}$ at large negative aileron deflections. (See figs. 8 and 9.) Of the configurations tested, the 500-pound spring in combination with the $0.48 \frac{c_b}{c_a}$ internal balance appears to have the most satisfactory stick force characteristics.

Extrapolation of the tab-angle curve (fig. 16) for the 28-pound spring and $0.48 \frac{c_b}{c_a}$ internal balance shows that all available tab deflection is used at 12.5° aileron deflection resulting in a maximum stick force only a few pounds less than for the 500-pound spring with the same balance. (See fig. 12.)

Although various spring stiffnesses were tested in conjunction with the $0.44 \frac{c_b}{c_a}$ internal balance, stick forces and rates of roll for these configurations are not presented because the maximum stick force for the lightest spring tested (28 lb/in.) was much greater than the maximum force allowable. The same general

stick-force gradient with total aileron angle was obtained with the $0.44 \frac{c_b}{c_a}$ internal balances. (See fig. 12.)

One method of eliminating the excessive stick forces for large deflections would be to replace the present aileron-stick linkage with a nonlinear linkage system. To show the advantage of such a system for this case, the nonlinear linkage shown in figure 14 was calculated by the method described in reference 4 and the stick forces were estimated for the $0.48 \frac{c_b}{c_a}$ balance with a 1000-pound-per-inch spring-tab stiffness at 300 miles per hour indicated airspeed. Figure 14 shows that the stick force for full deflection was reduced from 50 pounds to approximately 30 pounds with a negligible increase in stick force at lower deflections, giving a nearly linear variation of stick force with aileron deflection.

Rough estimates based on the variation of stick force with speed for the 500-pound-per-inch spring and $0.48 \frac{c_b}{c_a}$ balance indicate that such a system would be satisfactory throughout the speed range.

Rates of roll. - The calculated rates of roll were not corrected for the effects of wing twist and airplane yawing motion. The panel tested is the outboard section of the actual wing (fig. 2) and, therefore, some part of the effect of wing twist is included. The effect of the yawing motion would be small for most conditions calculated herein, as the angles of attack would be near the angle for zero lift. The calculated rates of roll (figs. 12 and 13) show that the maximum $pb/2V$ available with spring tab locked is approximately 0.092. Any reduction of stick forces by means of a spring tab will reduce the aileron effectiveness such that the $pb/2V$ requirements of reference 5 cannot be met. For the 500-pound spring in combination with the $0.48 \frac{c_b}{c_a}$ internal balance, reduction of the stick force to the desired value results in a $pb/2V$ of 0.078 which is 0.012 less than required in reference 5.

Although some flight data were available for comparison with the wind-tunnel results (fig. 15), the range covered (17.5° total aileron deflection) and the scatter of the data are such that no definite statement can be made concerning the agreement obtained. Considering the above fact and the difficulty in altering the existing model to obtain greater aileron effectiveness, no attempt

was made to modify the aileron configuration to get higher rates of roll pending correlations of the wind-tunnel tests with flight-test results in which greater aileron deflections are obtained.

The comparison of the requirements of reference 5 and the predicted rates of roll for the McDonnell XFD-1 airplane with the $0.48 \frac{c_b}{c_a}$ internal balance and the 500-pound-per-inch spring (fig. 18) shows that the lateral-control requirement will not be met in the speed range from 107 to 378 miles per hour indicated airspeed. The maximum deficiency in $pb/2V$ is 0.012 at 300 miles per hour indicated airspeed. This deficiency in rate of roll may be attributed to the high spring-tab deflections, and subsequent reductions in aileron rolling effectiveness for a given aileron deflection, necessary to reduce the stick forces to the required value.

Use of a nonlinear aileron-stick linkage system such as that described in the section "stick forces" would permit installation of a stiffer spring thus increasing the available $pb/2V$ for 30-pound stick force at 300 miles per hour indicated airspeed from 0.078 to approximately 0.083. This, coupled with modification of the present aileron system to permit approximately 3° more total aileron deflection, should bring the $pb/2V$ up to the required value of 0.09 at a stick force of about 33 pounds.

Spring-tab characteristics.- The variation of rolling-moment and aileron hinge-moment coefficients with tab deflection shown in figure 17 were determined by subtraction, at the same aileron angle and angle of attack, of the hinge-moment and rolling-moment coefficients for the spring tab locked from those with the spring tab operating. These data may be useful in estimating characteristics of other balance, spring-tab combinations for this aileron.

CONCLUSIONS

The results of the tests of the partial-span wing of the McDonnell XFD-1 airplane indicate the following:

1. Reduction of stick forces by use of the spring tab reduces the helix angle $pb/2V$ below the required value of 0.09.
2. Of the combinations tested, the one most satisfactory for obtaining a stick force of 30 pounds at 300 miles per hour indicated airspeed is the $0.48 \frac{c_b}{c_a}$ internal balance in combination with a

spring-tab stiffness of 500 pounds per inch. This combination gives a $pb/2V$ of 0.078.

Replacing the existing linear aileron-stick linkage with a nonlinear linkage would give a more satisfactory stick-force gradient with aileron deflection. This modification accompanied by modifications of the aileron system to permit an increase of approximately 3° total aileron travel should give the required helix angle $pb/2V$ of 0.09 for a stick force of approximately 33 pounds.

Langley Memorial Aeronautical Laboratory
National Advisory Committee for Aeronautics
Langley Field, Va.

Campbell C. Yates
Campbell C. Yates
Aeronautical Engineer

Leslie E. Schmitter
Leslie E. Schmitter
Aeronautical Engineer

Approved: *Joseph A. Shortell*
for Hartley A. Soule
Chief of Stability Research Division

ESY

APPENDIX

METHOD OF ESTIMATION OF STICK FORCES AND
RATES OF ROLL

Stick forces and rates of roll were estimated for the following conditions:

Weight of airplane, lb 9820
 Total aileron deflection, deg 30
 Stick travel for total aileron deflection, deg 22.75
 Stick length, ft 1.38
 Aileron-stick linkage Linear

Indicated airspeed (mph)	M	q (lb/ft ²)	Altitude (ft)
107	0.140	28.9	0
300	.475	230	10,000
378	.600	367	10,000

The stick forces and rates of roll were estimated by the general method of reference 6. The values of $\frac{C_{l_p}}{a_0} \sqrt{1 - M^2}$, a_0 , and C_{l_p} for the three conditions were as follows:

Indicated airspeed	$\frac{C_{l_p}}{a_0} \sqrt{1 - M^2}$ (reference 4)	a_0 (assumed)	C_{l_p}
107	3.80	0.106	0.407
300	3.54	.106	.426
378	3.40	.106	.450

The calculated rates of roll were not corrected for the effects of wing twist and airplane yawing motion

In several instances, the estimated angles of attack over the aileron section of the wing for the airplane in roll were outside the angle-of-attack range tested for that particular aileron deflection; the allowable loads on the balance system limiting the angle-of-attack range. To obtain the rolling-moment and hinge-moment data for the angle of attack for the wing in roll, the curves for the flap deflection in question were extrapolated by a straight line to the desired angle of attack.

To account for the differential aileron deflection with spring tabs operating, the following method was used to calculate the rate of roll and stick forces. The angle of attack and rolling-moment coefficients for various aileron deflections were first determined by the method of reference 6 assuming equal up and down aileron deflections. At the computed angle of attack for each aileron deflection the tab angle was determined from the test data. From the geometry of the system a change in aileron angle $\Delta\delta_a$, resulting from the deflection of the tab, was determined for each tab angle. The value $\Delta\delta_a$ represents the increased stick travel (in terms of aileron deflection) necessary to obtain the desired aileron deflection. Plots of $\delta_a + \Delta\delta_a$ versus δ_a (fig. 19) were then made for each spring configuration and for each air-speed. Values of up and down aileron deflection were determined from these curves at equal positive and negative values of $\delta_a + \Delta\delta_a$. The stick forces were then calculated as before.

For aileron deflections greater than 12° and -14° it was necessary to estimate the hinge-moment coefficient as consistent hinge-moment data could not be obtained during the tests. (See tests.) Estimates were made by determining the tab deflection corresponding to the desired δ_a from figure 16, and determining the value of ΔC_{h_a} for this tab angle from figure 17. This value was then deducted from the value of C_{h_a} for the same aileron deflection with spring tab locked 0° thus giving the value of C_{h_a} for the aileron with tab deflected.

For the tests in which data were taken at one angle of attack for each aileron deflection the rolling moments were assumed not to vary with angle of attack. Using this assumption, the angle of attack for a given δ_a was determined. The variation of C_{h_a} with α for the δ_a in question was estimated from other configurations and a line having this slope was drawn through the one point for the desired δ_a . This line was extended to the angle of attack estimated as previously described. As noted in the text, these tests were run only to gain some indication of what the final configuration might be.

REFERENCES

1. Thom, A.: Blockage Corrections and Chocking in the R.A.E. High Speed Tunnel. Rep. No. Aero 1891, British R.A.E., Nov. 1943.
2. Swanson, Robert S., and Toll, Thomas A.: Jet-Boundary Corrections for Reflection-Plane Models in Rectangular Wind Tunnels. NACA ARR No. 3E22, 1943.
3. Mendelsohn, Robert A.: Wind-Tunnel Tests to Determine Aileron Characteristics of a 0.3-Scale Partial-Span Model of a Fleetwings XBTk-1 Wing Panel - TED No. NACA 2334. NACA MR No. L5F16, Bur. Aero., 1945.
4. Lowry, John G.: Adjustment of Stick Force by a Nonlinear Aileron-Stick Linkage. NACA RB, Nov. 1942.
5. Anon.: Specification for Stability and Control Characteristics of Airplanes. SR-119A, Bur. Aero., April 7, 1945.
6. Swanson, Robert S., and Priddy, E. LaVerne: Lifting-Surface-Theory Values of the Damping in Roll and of the Parameter Used in Estimating Aileron Stick Forces. NACA ARR No. L5F23, 1945.

TABLE I

GEOMETRIC CHARACTERISTICS OF THE MCDONNELL XFD-1 PARTIAL-SPAN
AND FULL-SPAN WING

	Partial-span wing	Full-span wing
Wing:		
Area, sq ft	42.48	273.74
Span, ft	8.45	40.77
Mean aerodynamic chord, ft	5.51	7.08
Aspect ratio	3.36	6.07
Taper ratio	0.66	0.445
Airfoil section:		
Theoretical tip	NACA 66(215)-414 (a = 0.6)	
Theoretical root at center line of airplane	NACA 66,2-218 (a = 0.6)	
Aileron (same for partial-span and full-span wing):		
Area (one aileron),sq ft		8.31
Span, along hinge line, ft		7.28
Root-mean-square chord, ft		1.13
Hinge-line location, percent of wing chord		78.8
Spring tab (same for partial-span and full-span wing):		
Area, sq ft		0.94
Span, along hinge line, ft		3.43
Root-mean-square chord, ft		0.27
Hinge-line location, percent of aileron chord		24.23

CONFIDENTIAL

FIGURE LEGENDS

Figure 1.- Full-scale partial-span wing of the McDonnell XFD-1 airplane.

Figure 2.- General arrangement of the McDonnell XFD-1 airplane.

Figure 3.- Inboard and outboard ends of 44-percent aileron balance on McDonnell XFD-1 airplane.

Figure 4.- Inboard and outboard ends of 48-percent aileron balance on McDonnell XFD-1 airplane.

Figure 5.- Aileron spring tab linkage in the McDonnell XFD-1 airplane.

Figure 6.- McDonnell XFD-1 partial-span wing mounted in Langley high-speed 7- by 10-foot tunnel.

(a) Looking upstream.

Figure 6.- Concluded.

(b) Looking downstream.

Figure 7.- Schematic sketch of method used to determine the seal leakage factor.

Figure 8.- Pressure coefficient across seal of internal balance on McDonnell XFD-1 airplane with 44 percent internal balance.

(a) Spring tab blocked, $M = 0.416$, $q = 229 \text{ lb/ft}^2$.

Figure 8.- Concluded.

(b) 28 lb/in. spring, $M = 0.416$, $q = 228 \text{ lb/ft}^2$.

Figure 9.- Pressure coefficient across seal of internal balance on McDonnell XFD-1 airplane with 48 percent internal balance.

(a) Spring tab blocked, $M = 0.416$, $q = 229 \text{ lb/ft}^2$.

Figure 9.- Continued.

(b) 500 lb/in. spring, $M = 0.630$, $q = 459 \text{ lb/ft}^2$.

Figure 9.- Continued.

(c) 500 lb/in. spring, $M = 0.416$, $q = 229 \text{ lb/ft}^2$.

CONFIDENTIAL

FIGURE LEGENDS - Continued

Figure 9.- Concluded.

(d) 500 lb/in. spring, $M = 0.146$, $q = 31 \text{ lb/ft}^2$.

Figure 10.- Aileron hinge-moment characteristics of the wing of McDonnell XFD-1 airplane with 44 percent internal balance.

(a) Spring tab blocked, $M = 0.416$, $q = 229 \text{ lb/ft}^2$.

Figure 10.- Continued.

(b) 28 lb/in. spring, $M = 0.416$, $q = 228 \text{ lb/ft}^2$.

Figure 10.- Concluded.

(c) 500 lb/in. spring, $M = 0.417$, $q = 228 \text{ lb/ft}^2$.

Figure 11.- Aileron hinge and rolling moment characteristics of the McDonnell XFD-1 airplane with 48 percent internal balance.

(a) Spring tab blocked, $M = 0.416$, $q = 229 \text{ lb/ft}^2$.

Figure 11.- Continued.

(b) 28 lb/in. spring, $M = 0.416$, $q = 229 \text{ lb/ft}^2$.

Figure 11.- Continued.

(c) 500 lb/in. spring, $M = 0.416$, $q = 229 \text{ lb/ft}^2$.

Figure 11.- Continued.

(d) 500 lb/in. spring, $M = 0.630$, $q = 459 \text{ lb/ft}^2$.

Figure 11.- Continued.

(e) 500 lb/in. spring, $M = 0.146$, $q = 31 \text{ lb/ft}^2$.

Figure 11.- Concluded.

(f) 1500 lb/in. spring, $M = 0.417$, $q = 229 \text{ lb/ft}^2$.

Figure 12.- Variation of stick force and wing-tip helix angle with aileron deflection for several combinations of internal balance and spring tab stiffness. Indicated airspeed = 300 mph, $M = 0.475$.

FIGURE LEGENDS - Concluded

- Figure 13.- Variation of stick force and wing-tip helix angle with aileron deflection for several indicated airspeeds. $c_b/c_a = 0.48$, 500 lb/in. spring.
- Figure 14.- Linkage and stick force characteristics for nonlinear aileron-stick linkage.
- Figure 15.- Comparison of estimated aileron characteristics with those obtained in airplane flight tests. Spring tab blocked, $c_b/c_a = 0.44$, indicated airspeed = 200 mph.
- Figure 16.- Variation of spring-tab deflection with aileron deflection in steady roll.
- Figure 17.- Variation of hinge- and rolling-moment coefficient with spring tab deflection.
- Figure 18.- Comparison of Navy rate of roll requirement and predicted rate of roll of McDonnell XFD-1 airplane with $c_b/c_a = 0.48$, 500 lb/in. spring.
- Figure 19.- Typical plot of $\delta_a + \Delta\delta_a$ versus aileron angle for determination of aileron angles with differential resulting from spring tab operation.

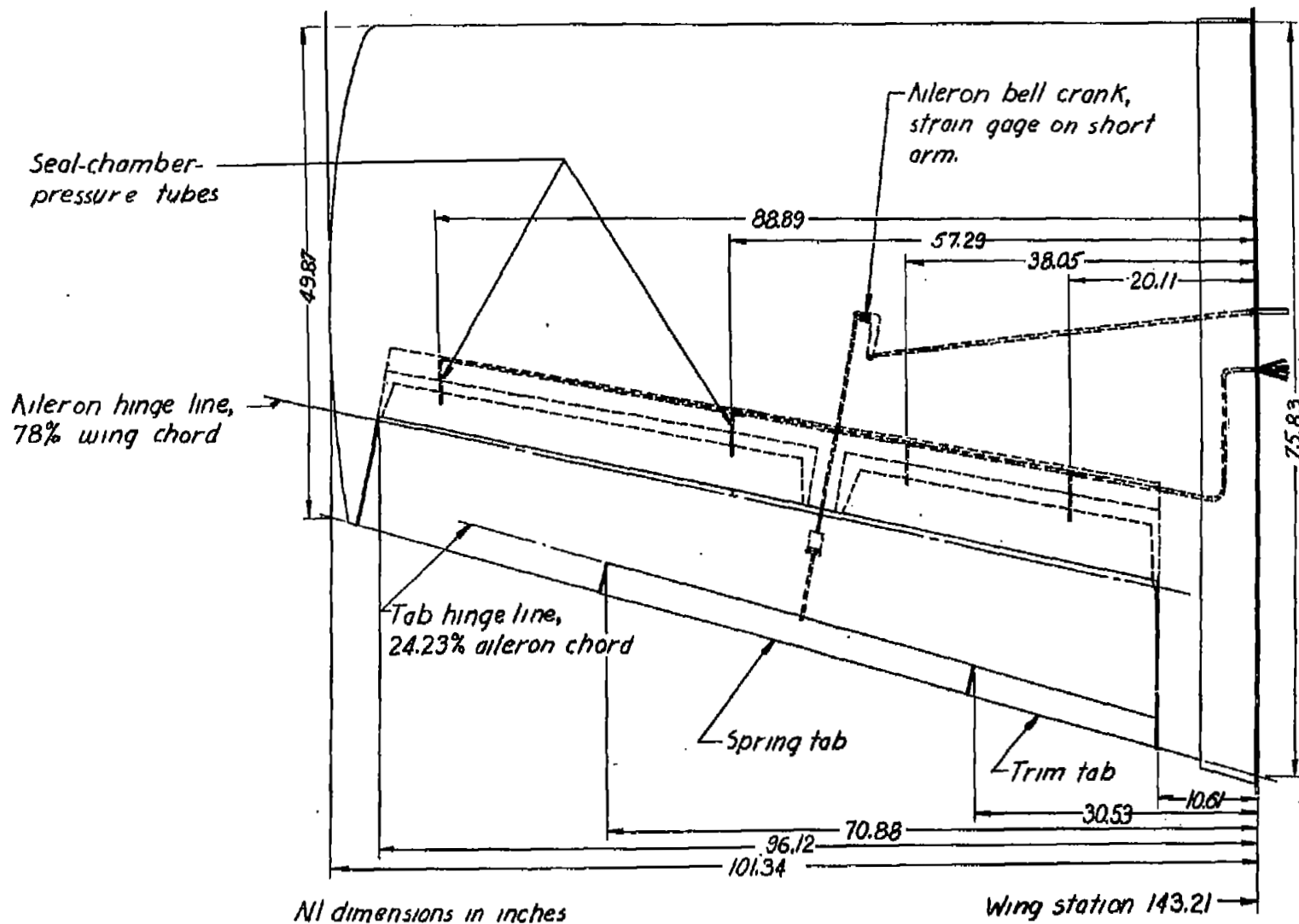
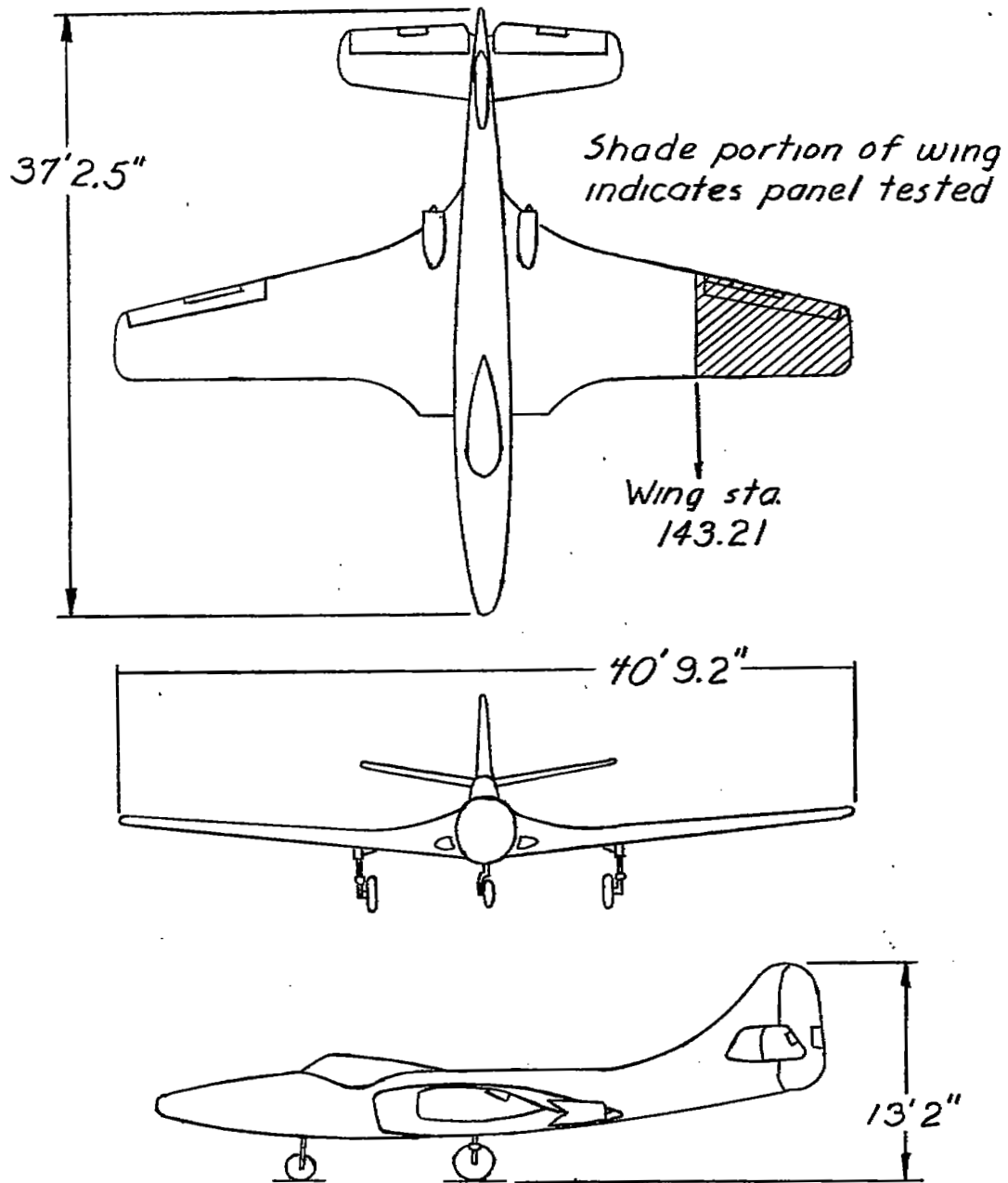


Figure 1.-Full-scale partial-span wing of the McDonnell XFD-1 airplane.

NATIONAL ADVISORY
COMMITTEE FOR AERONAUTICS



NATIONAL ADVISORY
COMMITTEE FOR AERONAUTICS

Figure 2.- General arrangement of the
McDonnell XFD-1 airplane.

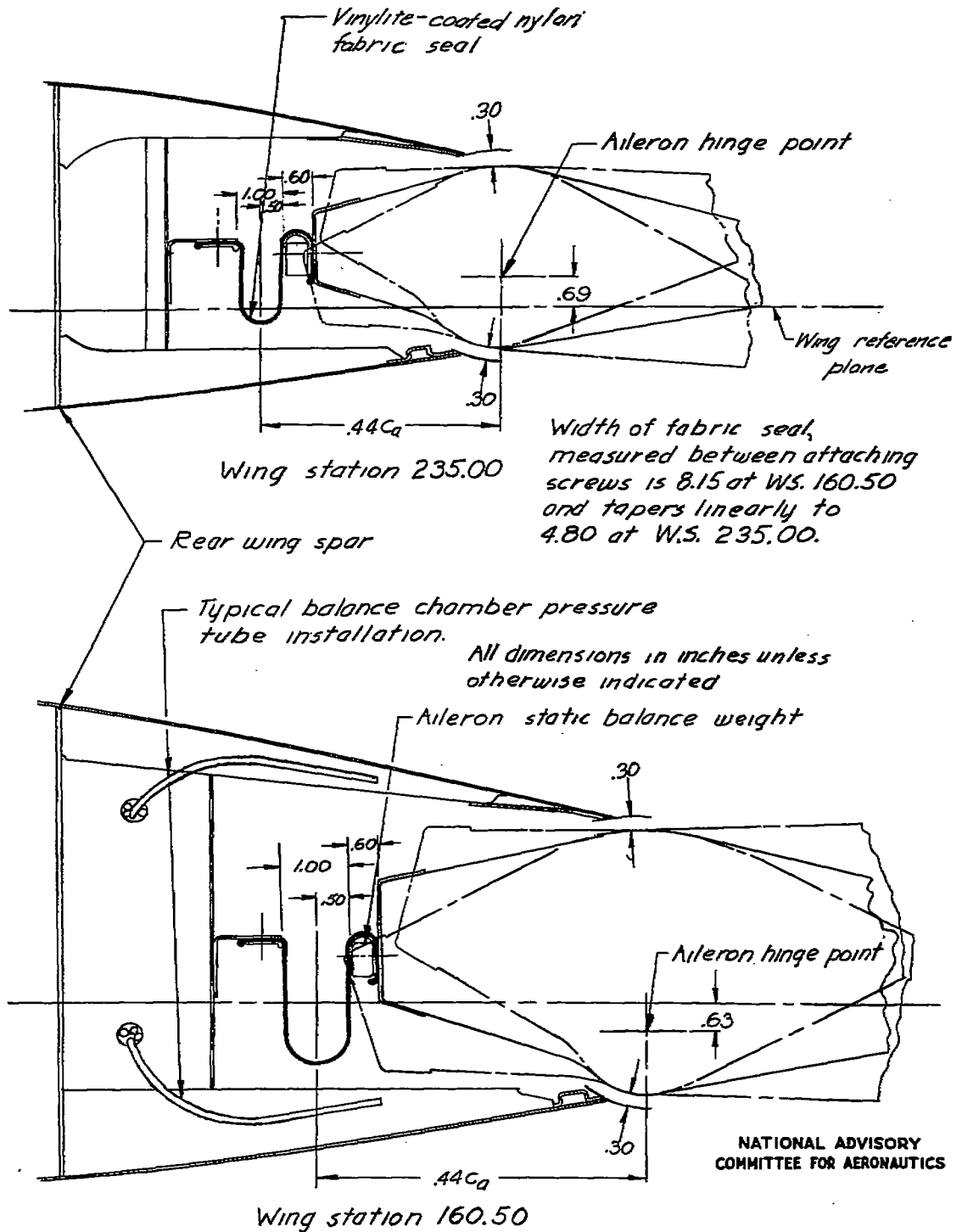


Figure 3-Inboard and outboard ends of 44-percent aileron balance on McDonnell XF-1 airplane. 1886

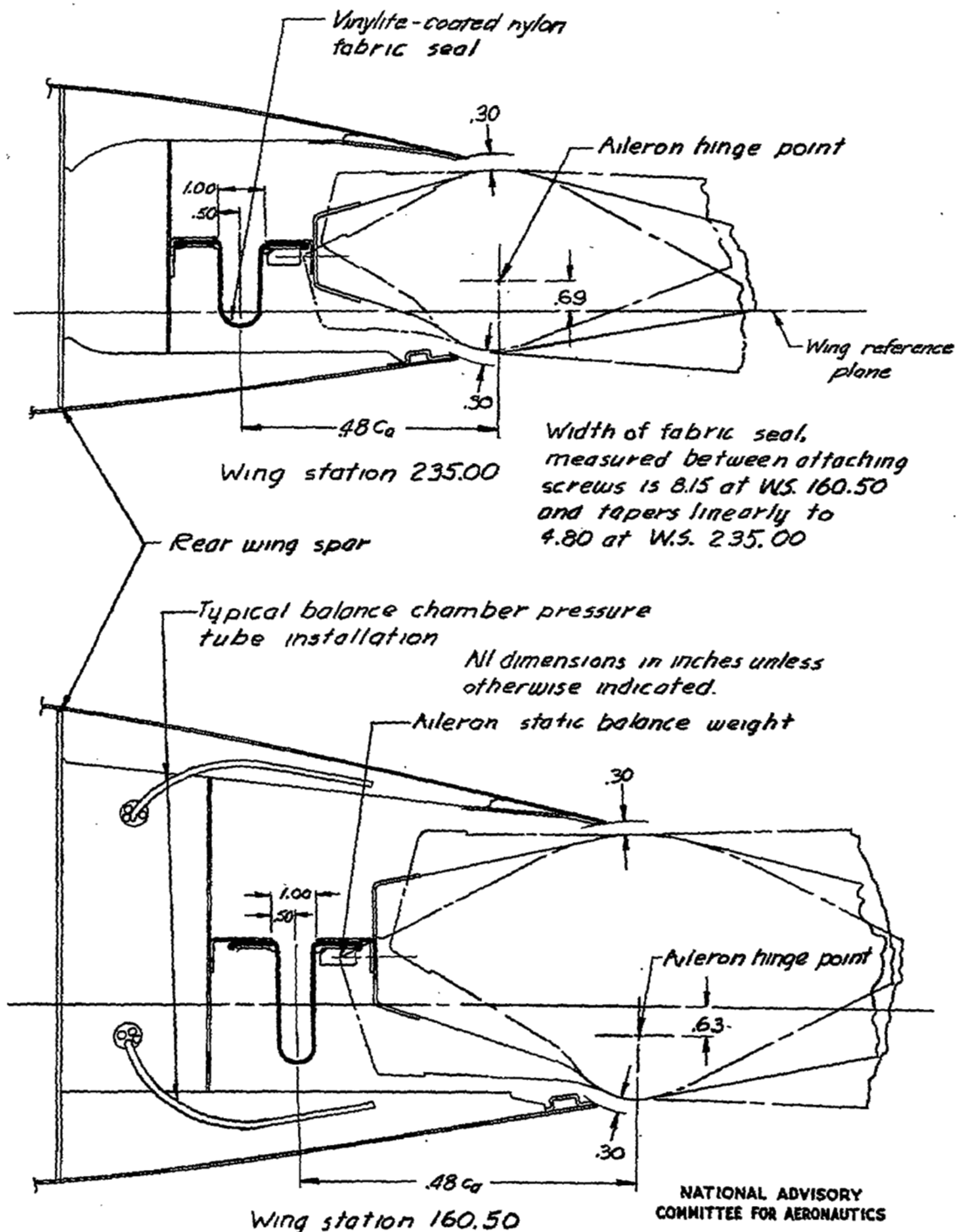


Figure 4.- Inboard and outboard ends of 48-percent aileron balance on McDonnell XFD-1 airplane

1008 5

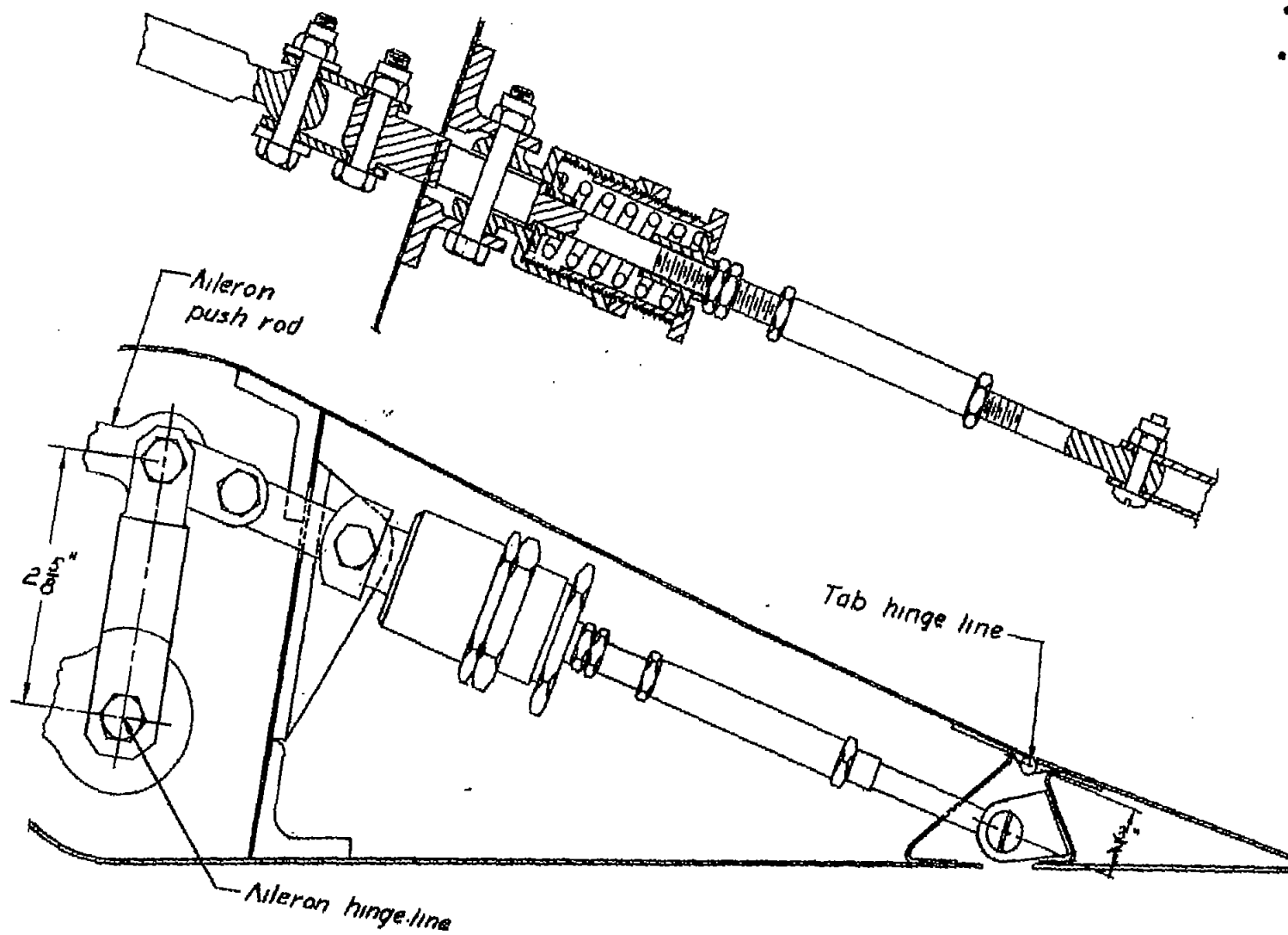
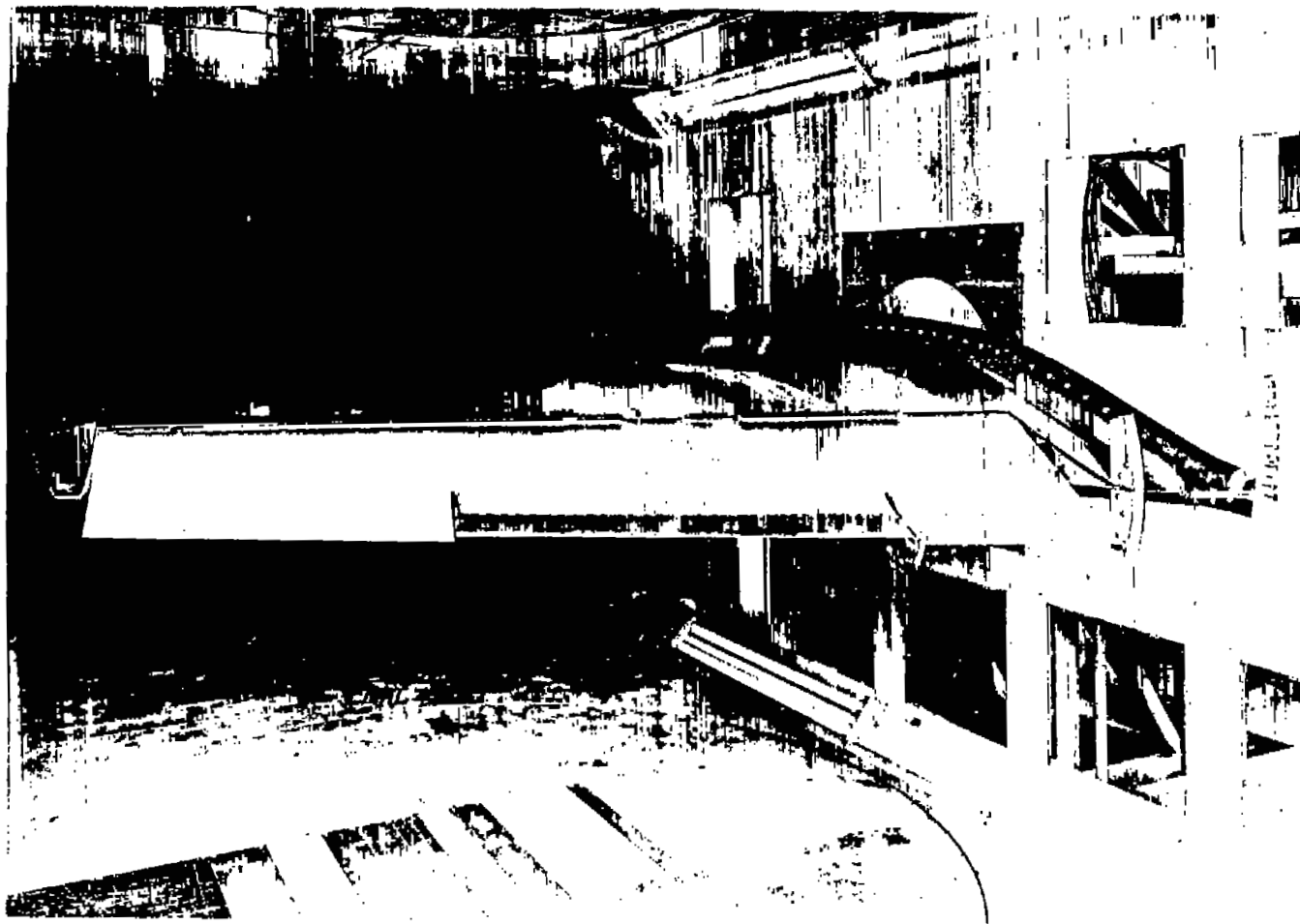


Figure 5.- Aileron spring tab linkage in the McDonnell XFD-1 airplane.

NATIONAL ADVISORY
COMMITTEE FOR AERONAUTICS

NACA RM No. 16H21a



(a) Looking upstream.

Figure 6.- McDonnell XFD-1 partial-span wing mounted
in Langley high-speed 7- by 10-foot tunnel.

NACA RM No. 16H21a



(b) Looking downstream.

Figure 6.- Concluded.

NATIONAL ADVISORY COMMITTEE FOR AERONAUTICS
LANGLEY MEMORIAL AERONAUTICAL LABORATORY - LANGLEY FIELD, VA.

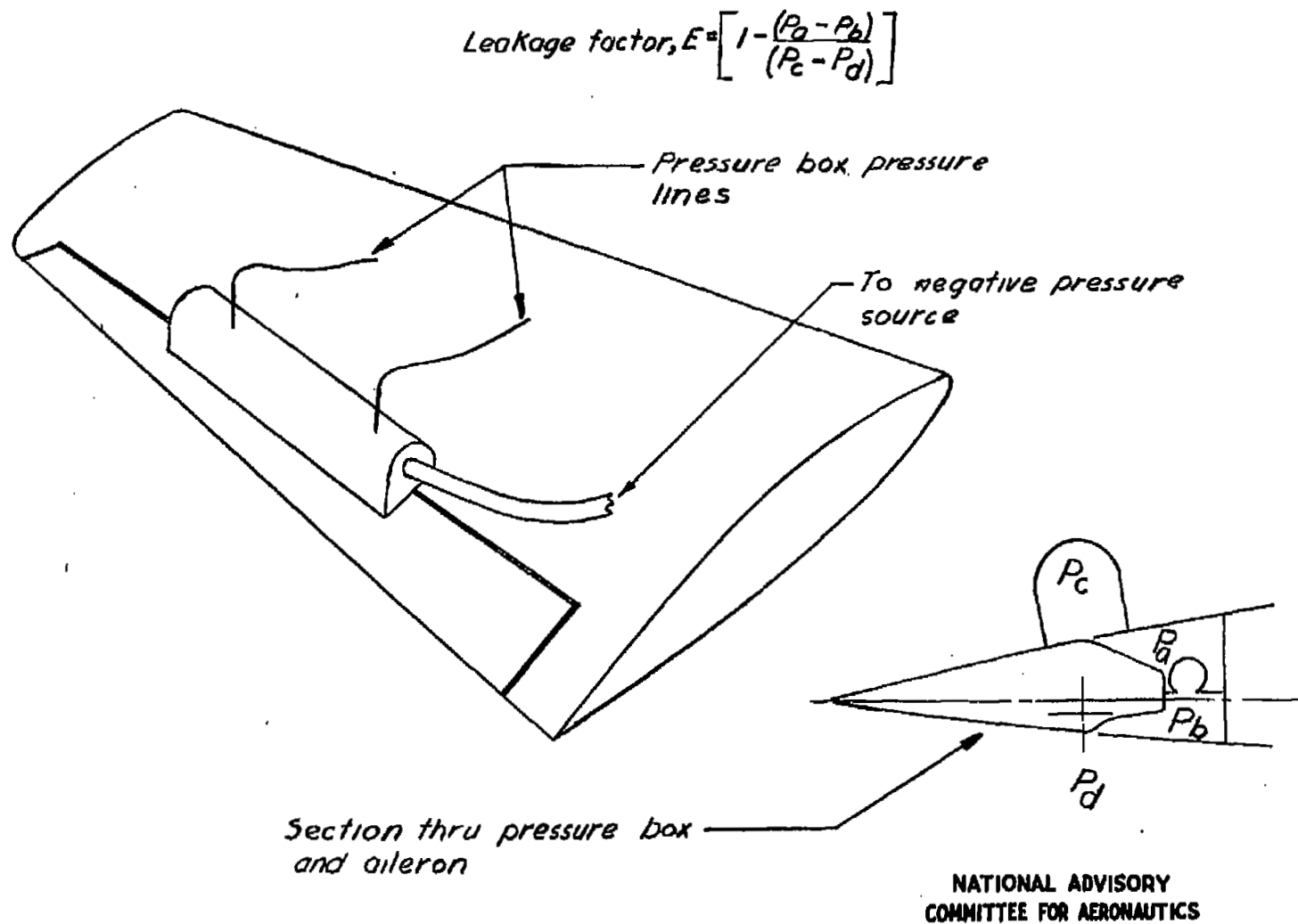
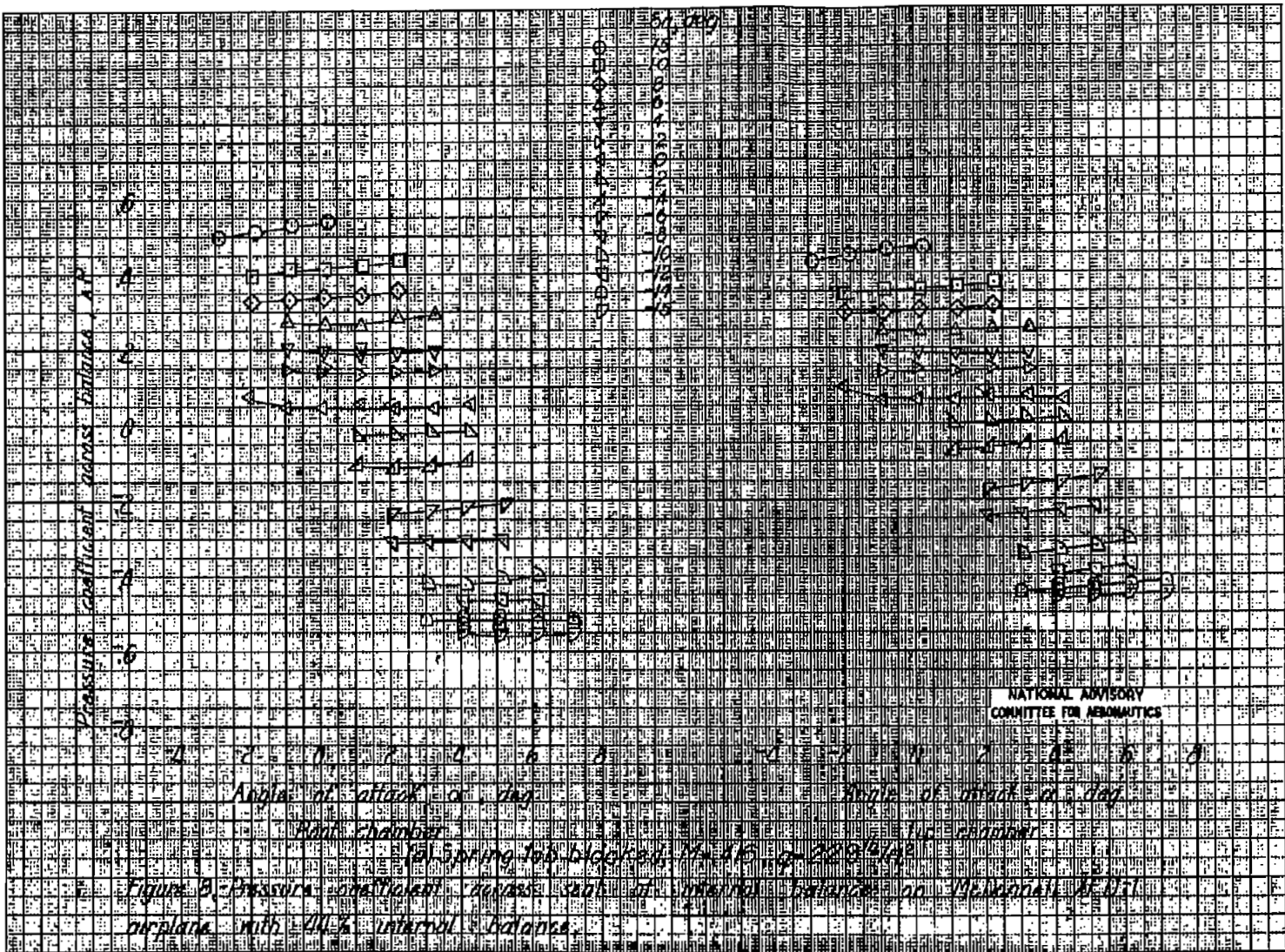
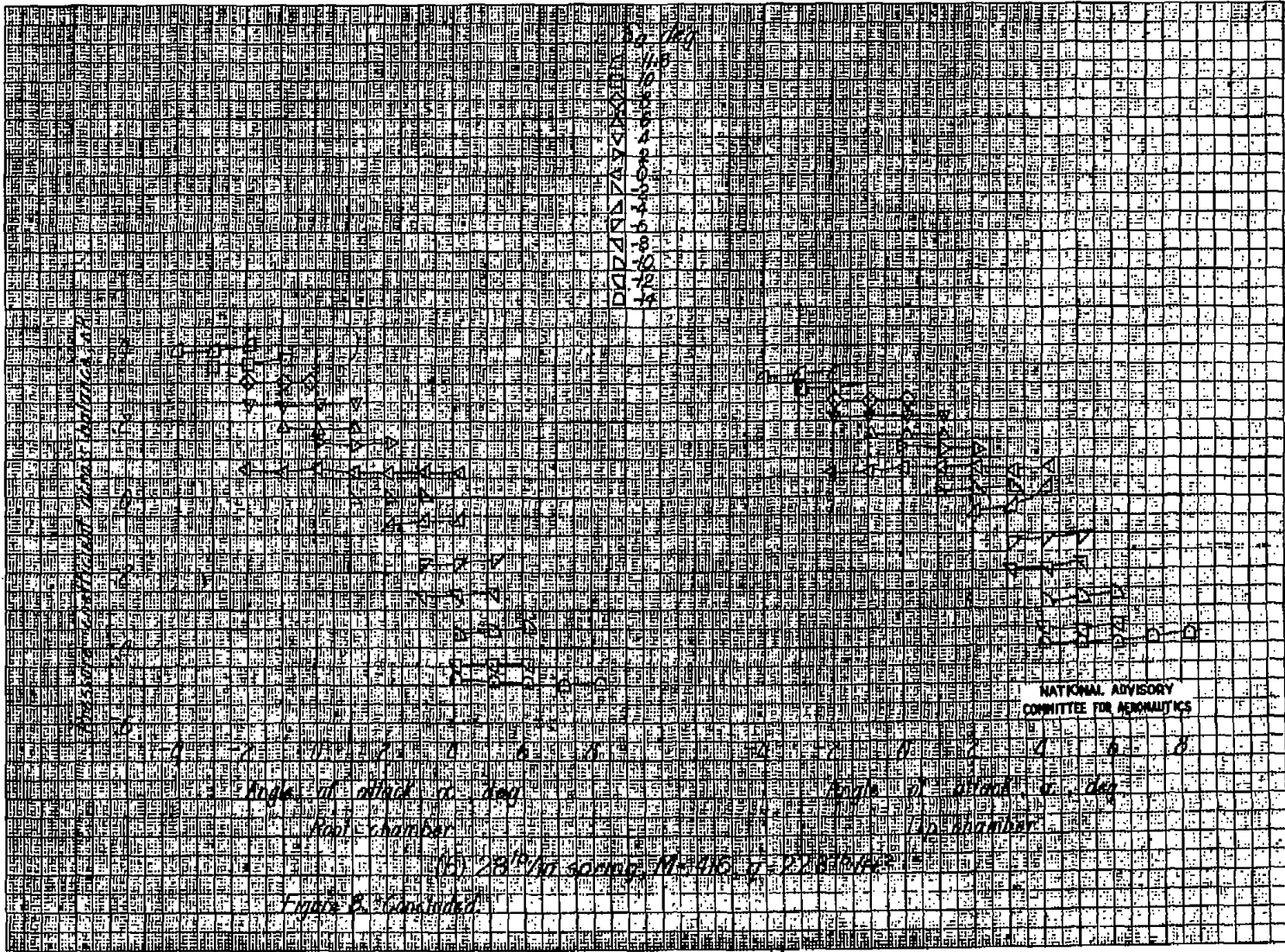
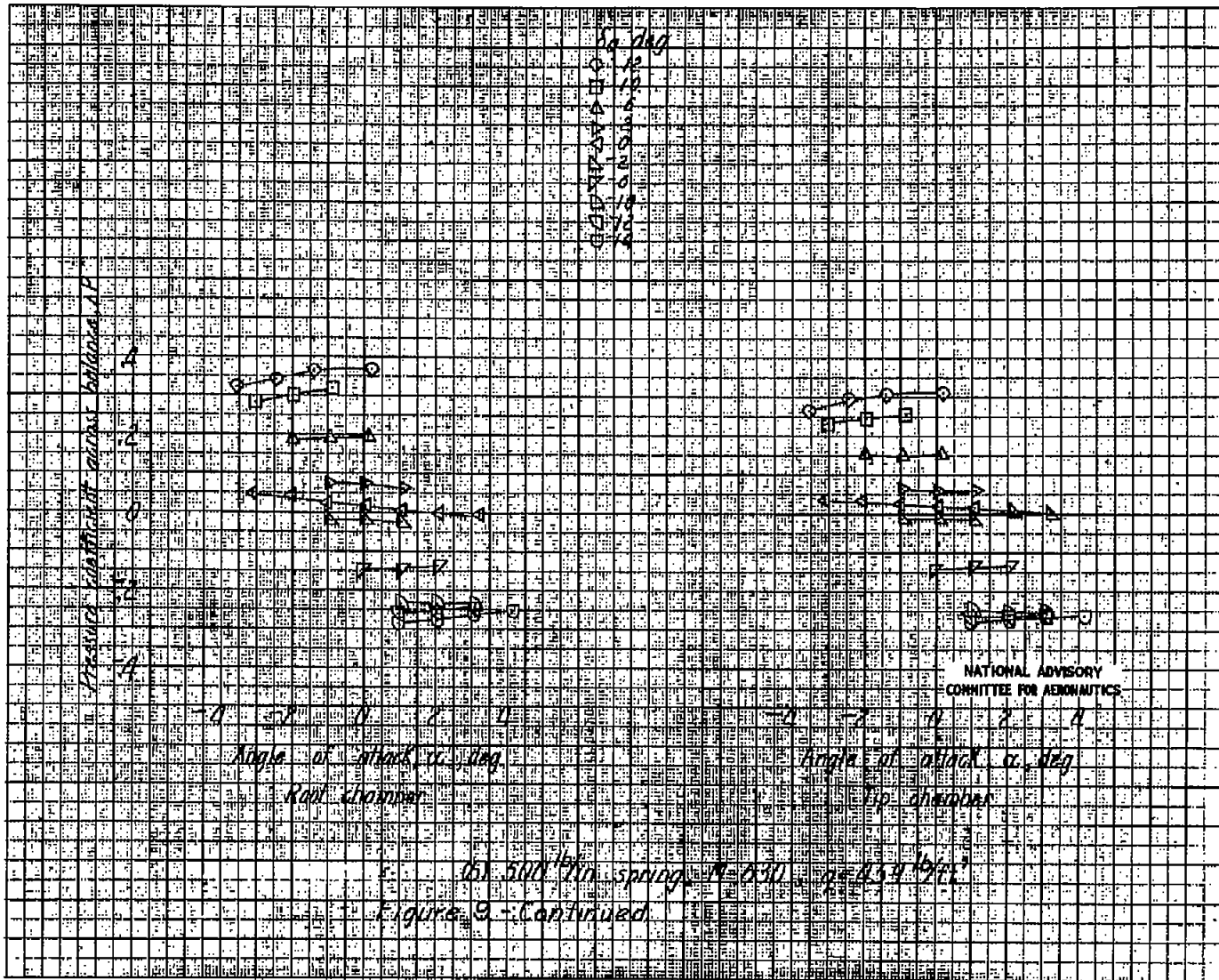
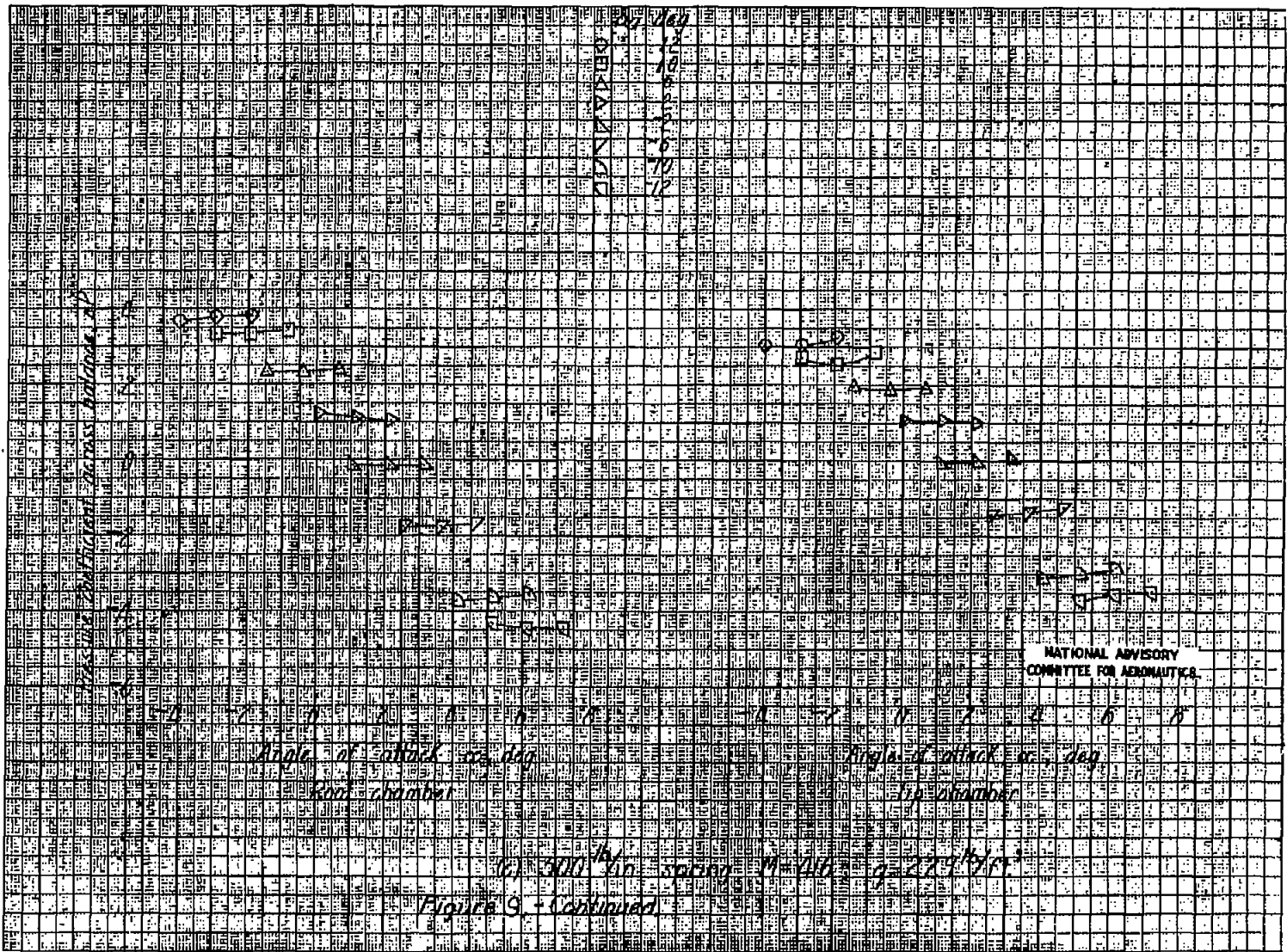


Figure 7.- Schematic sketch of method used to determine the seal leakage factor.

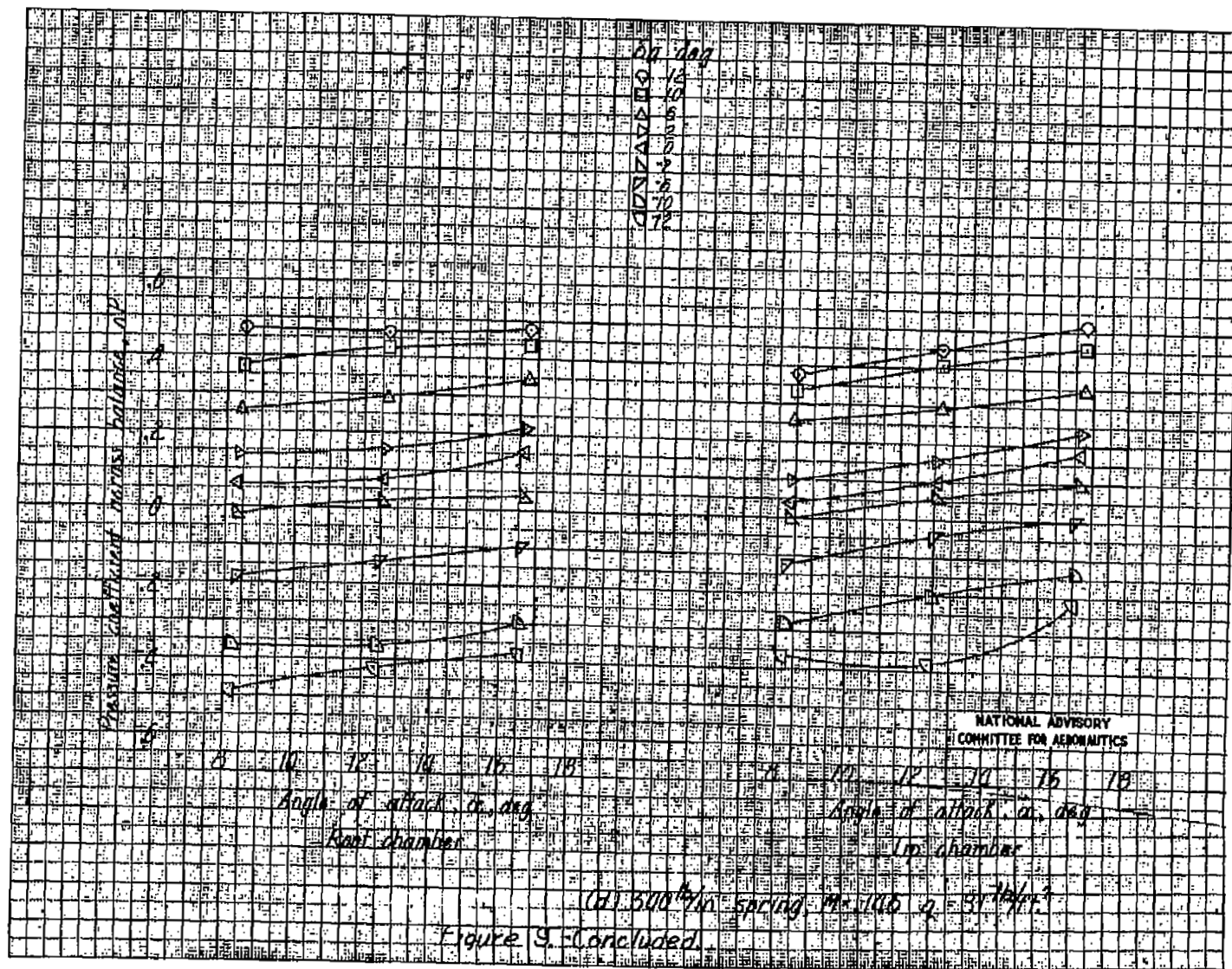


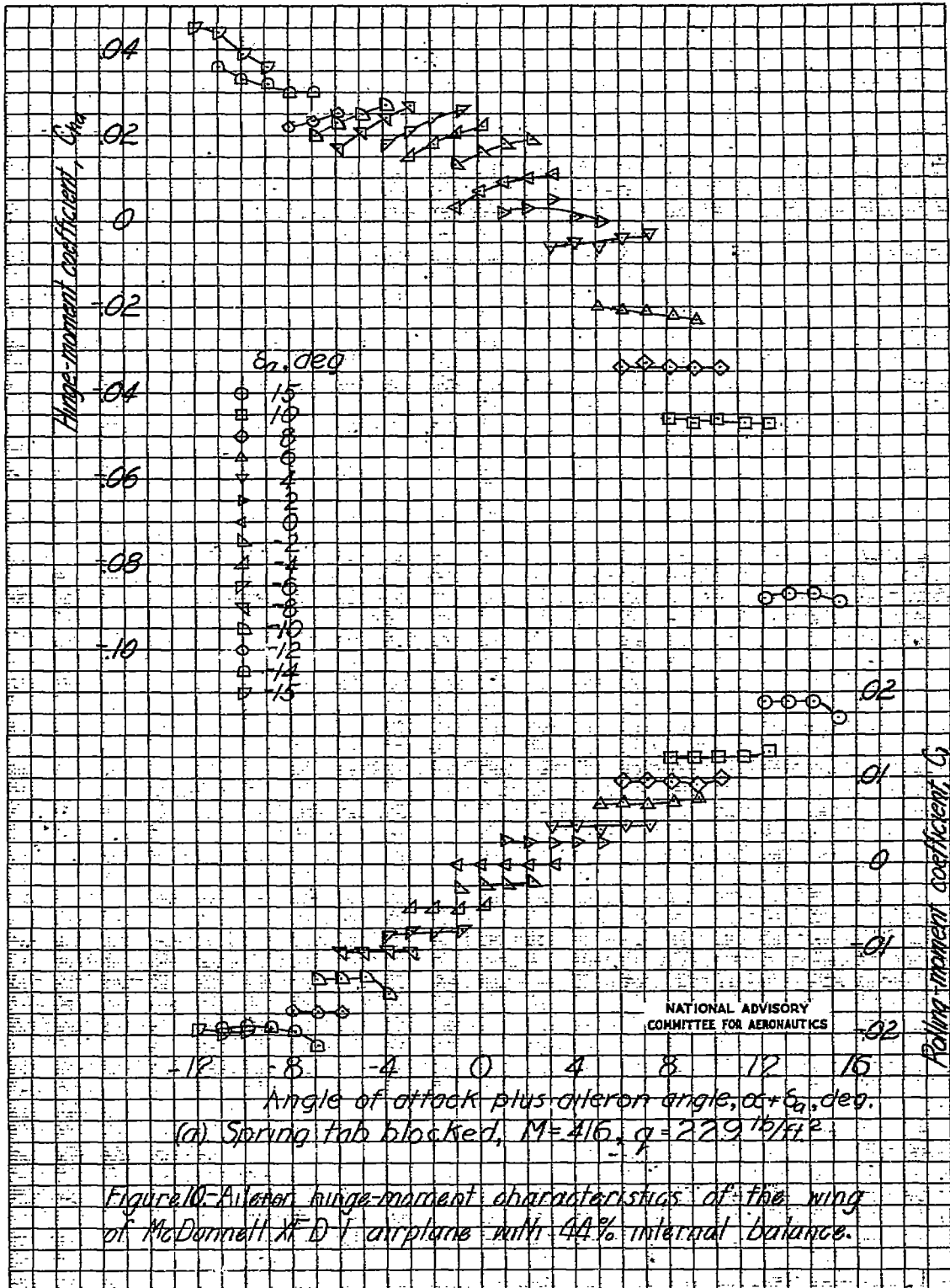


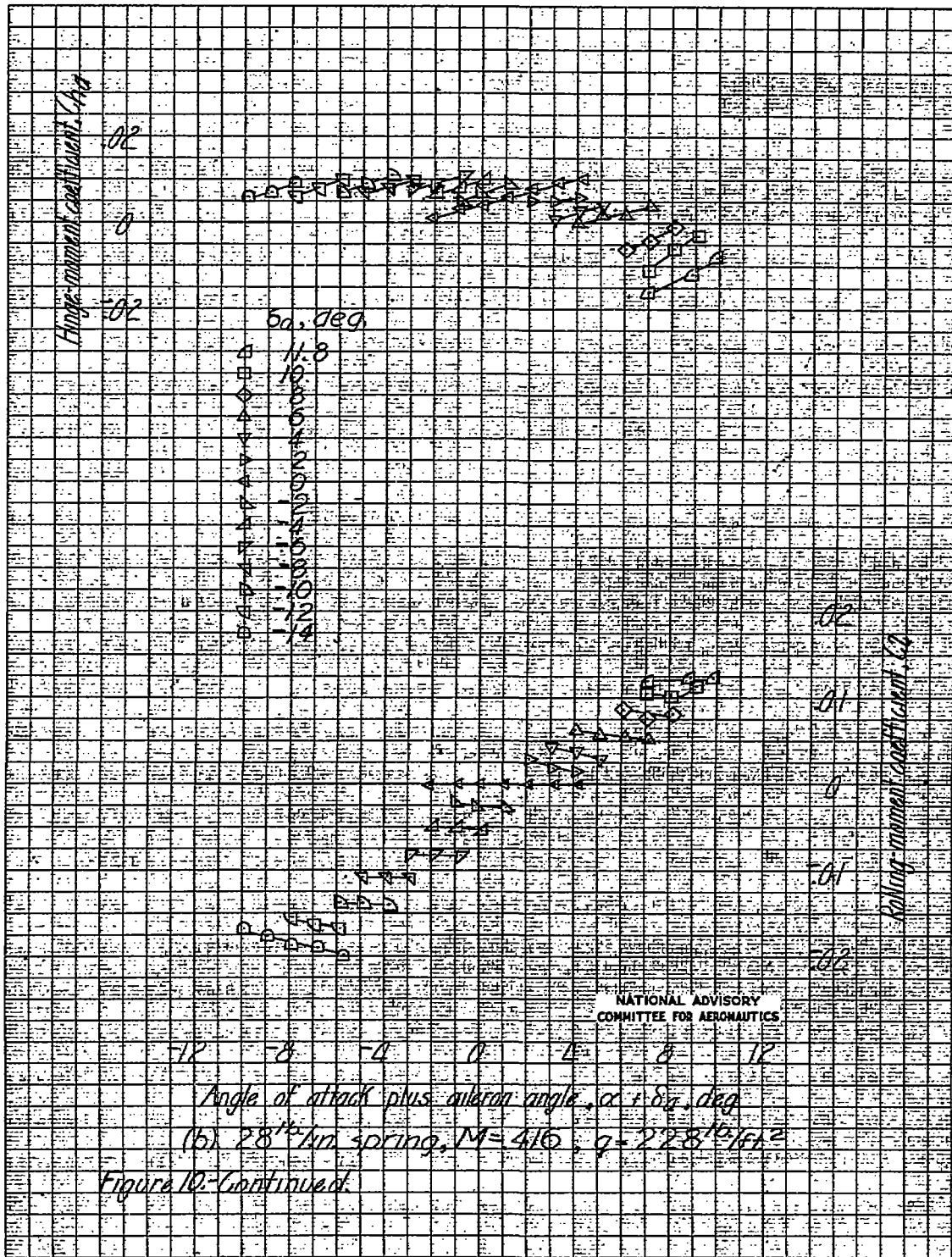




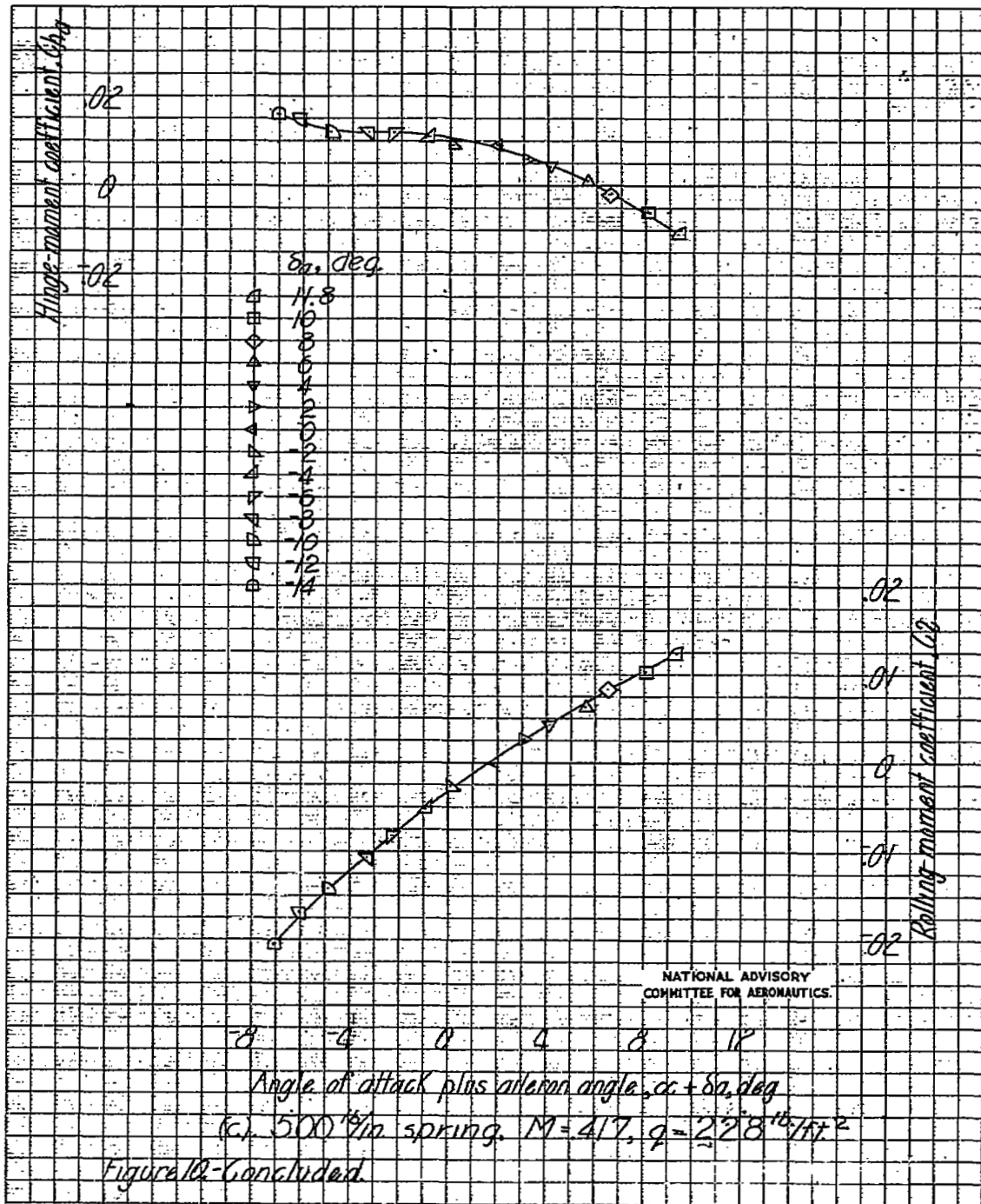
NATIONAL ADVISORY
COMMITTEE FOR AERONAUTICS

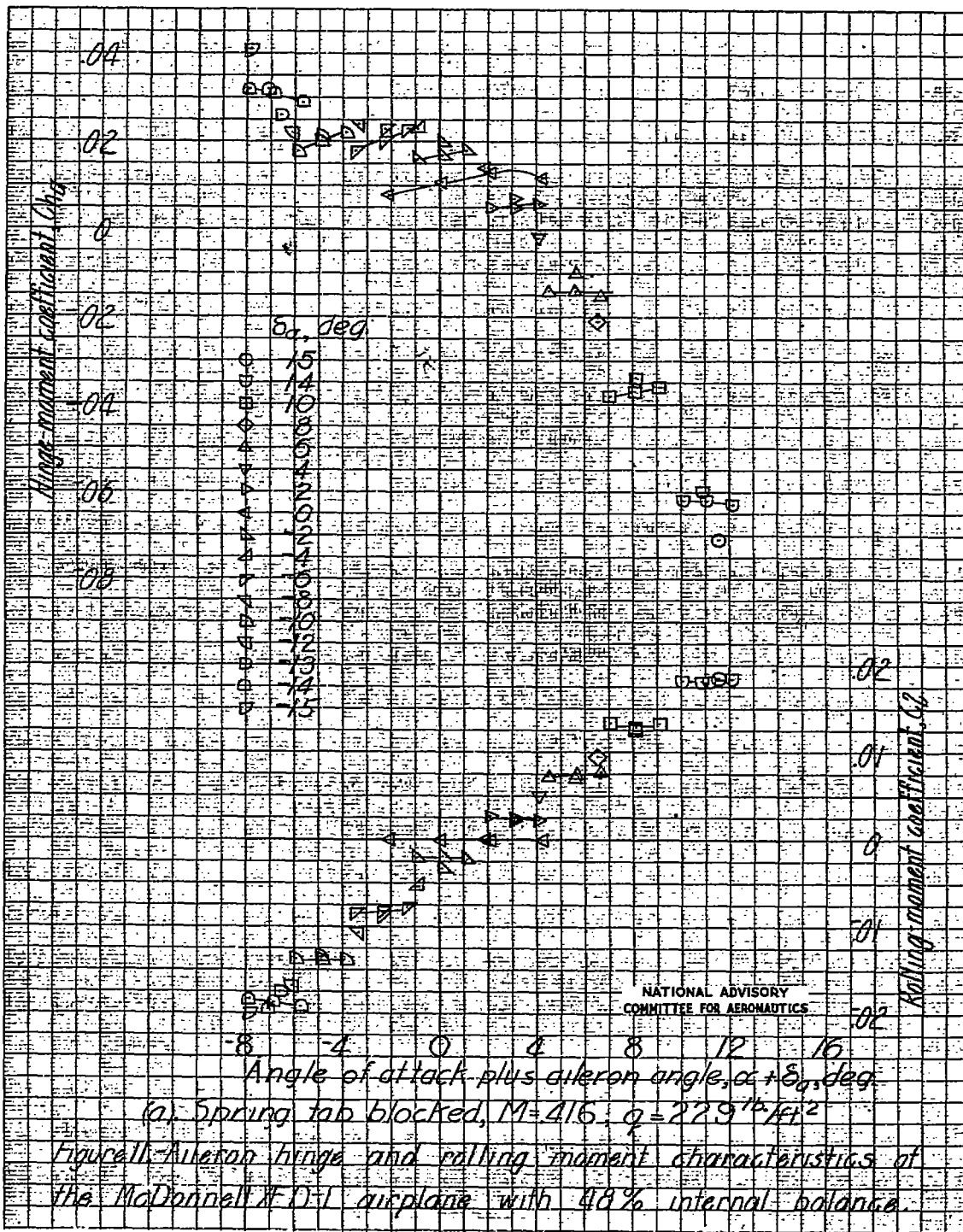


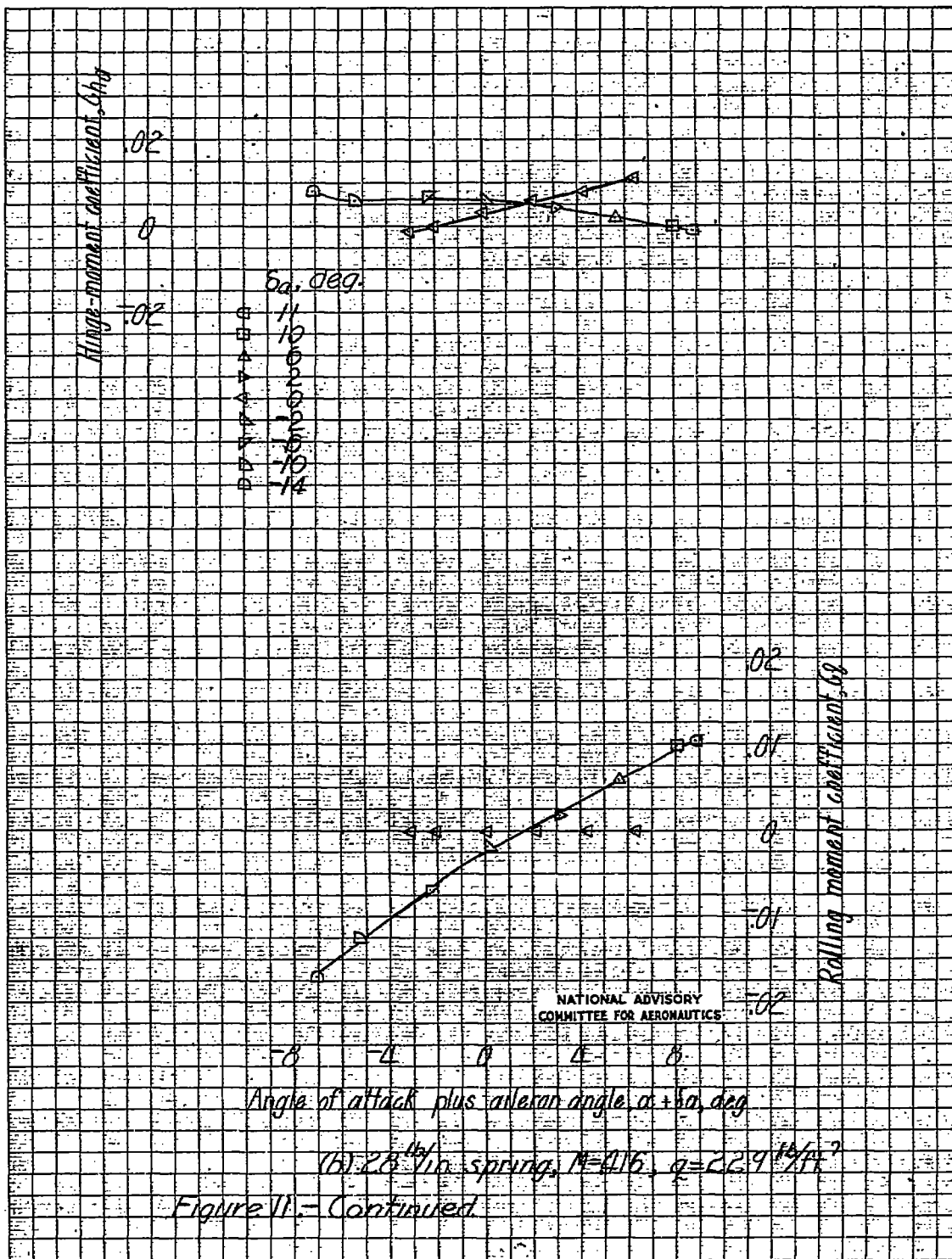


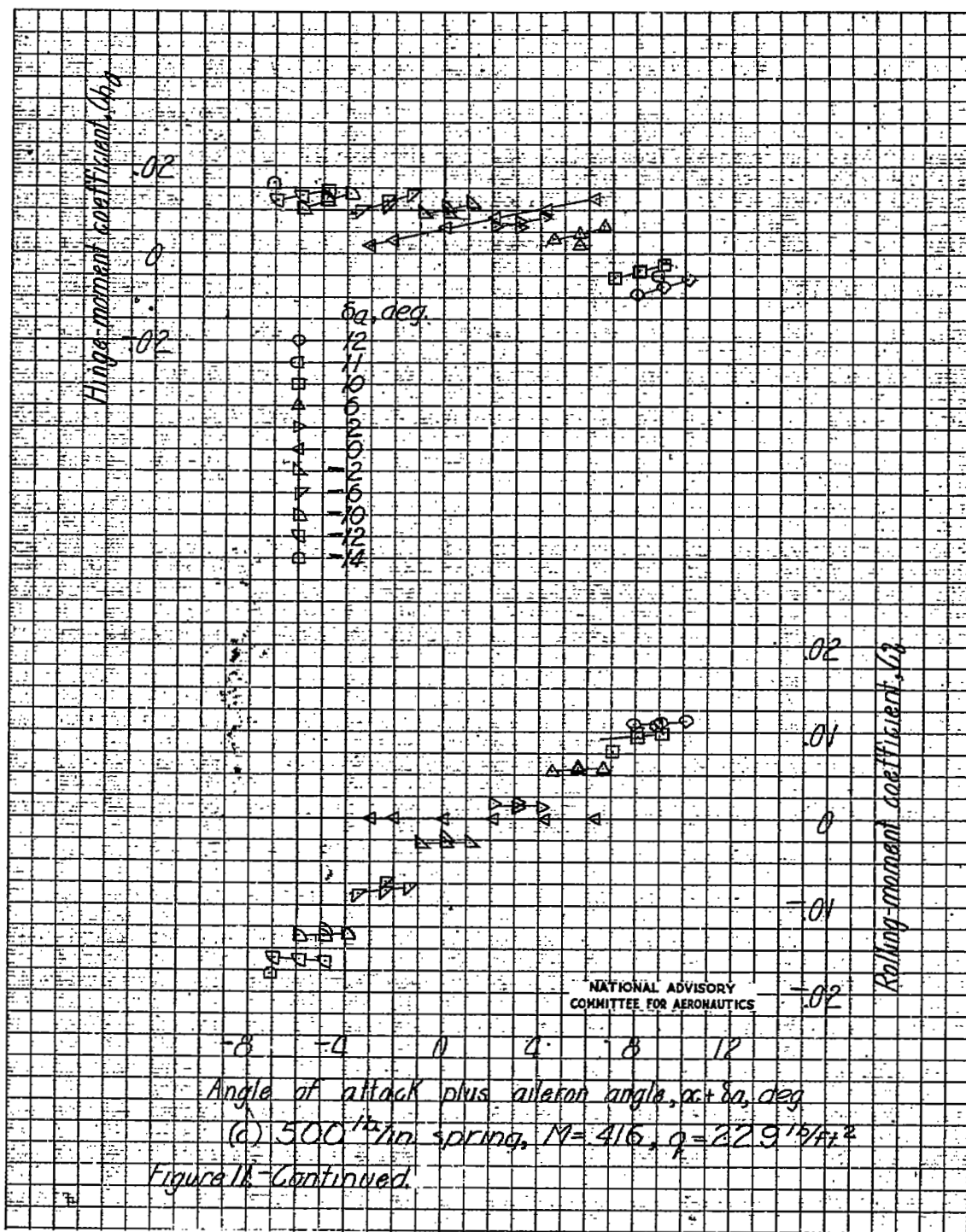


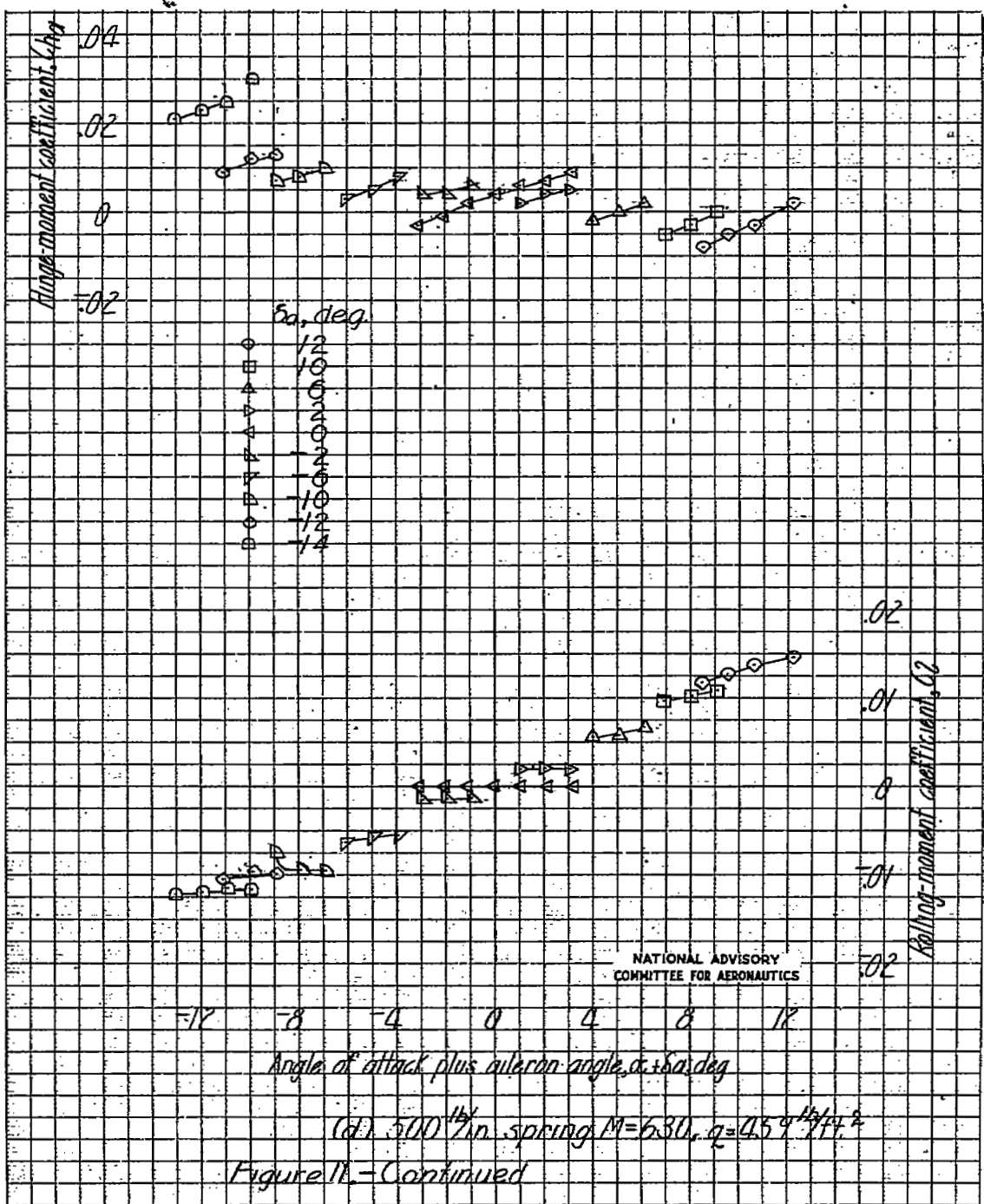
198610

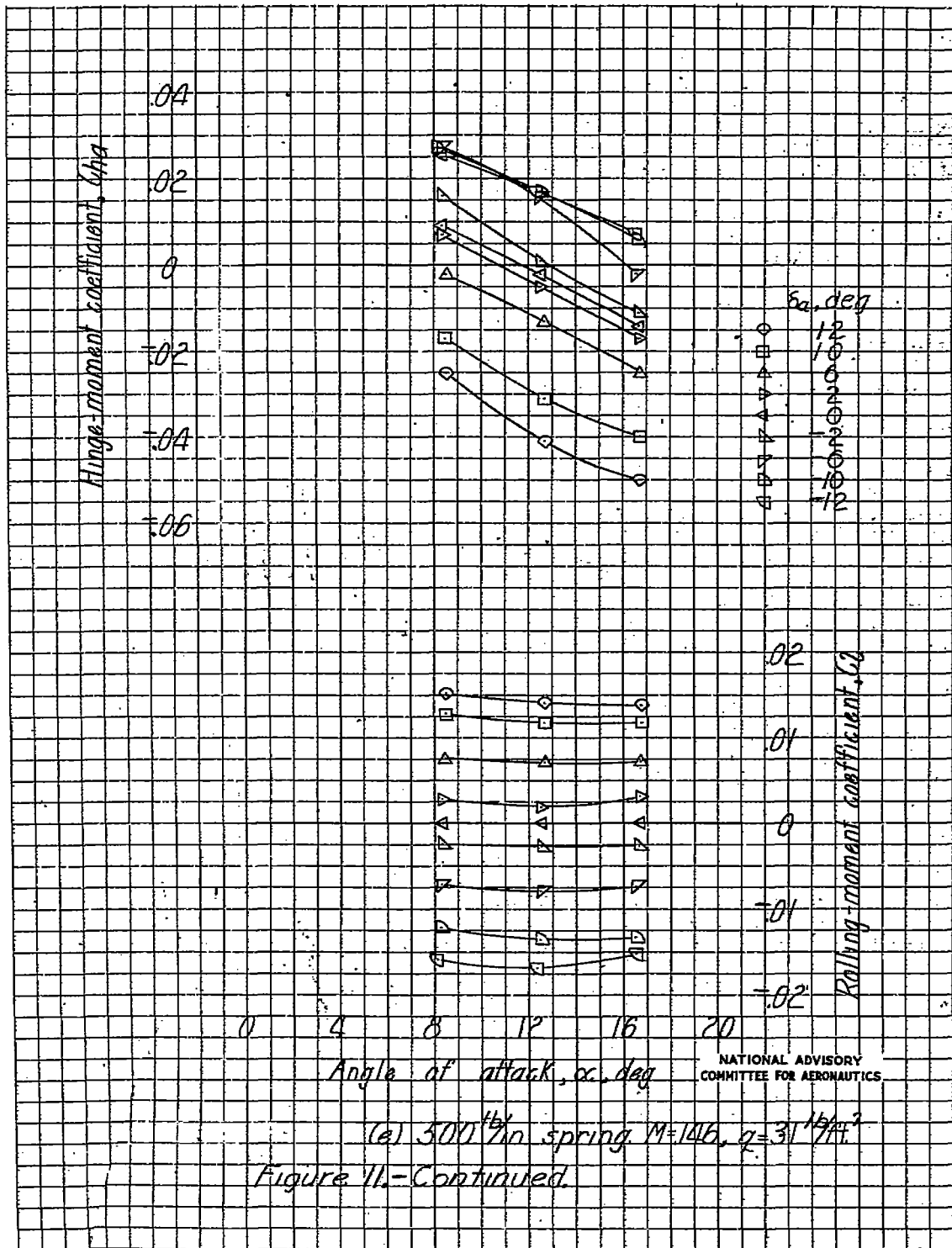


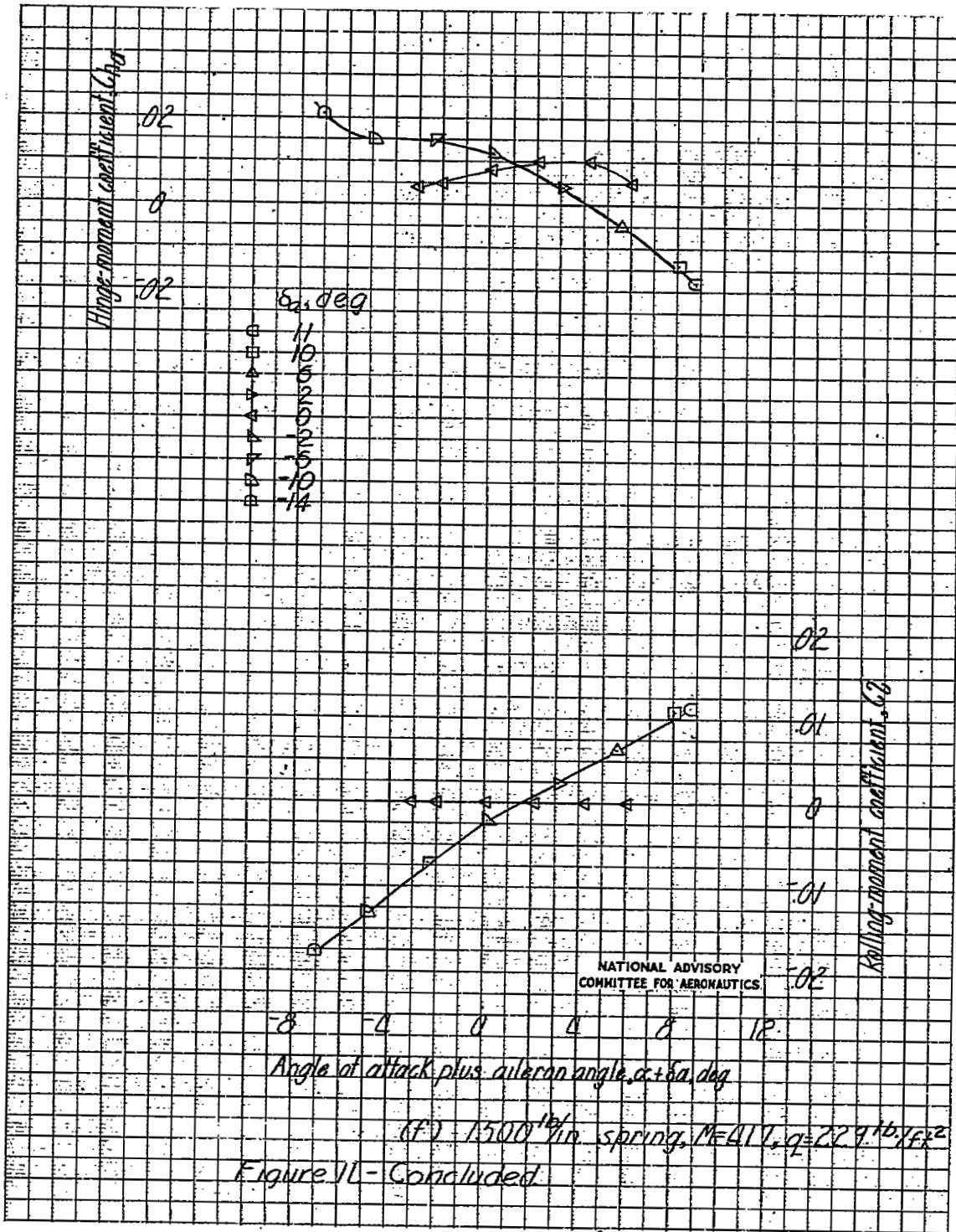












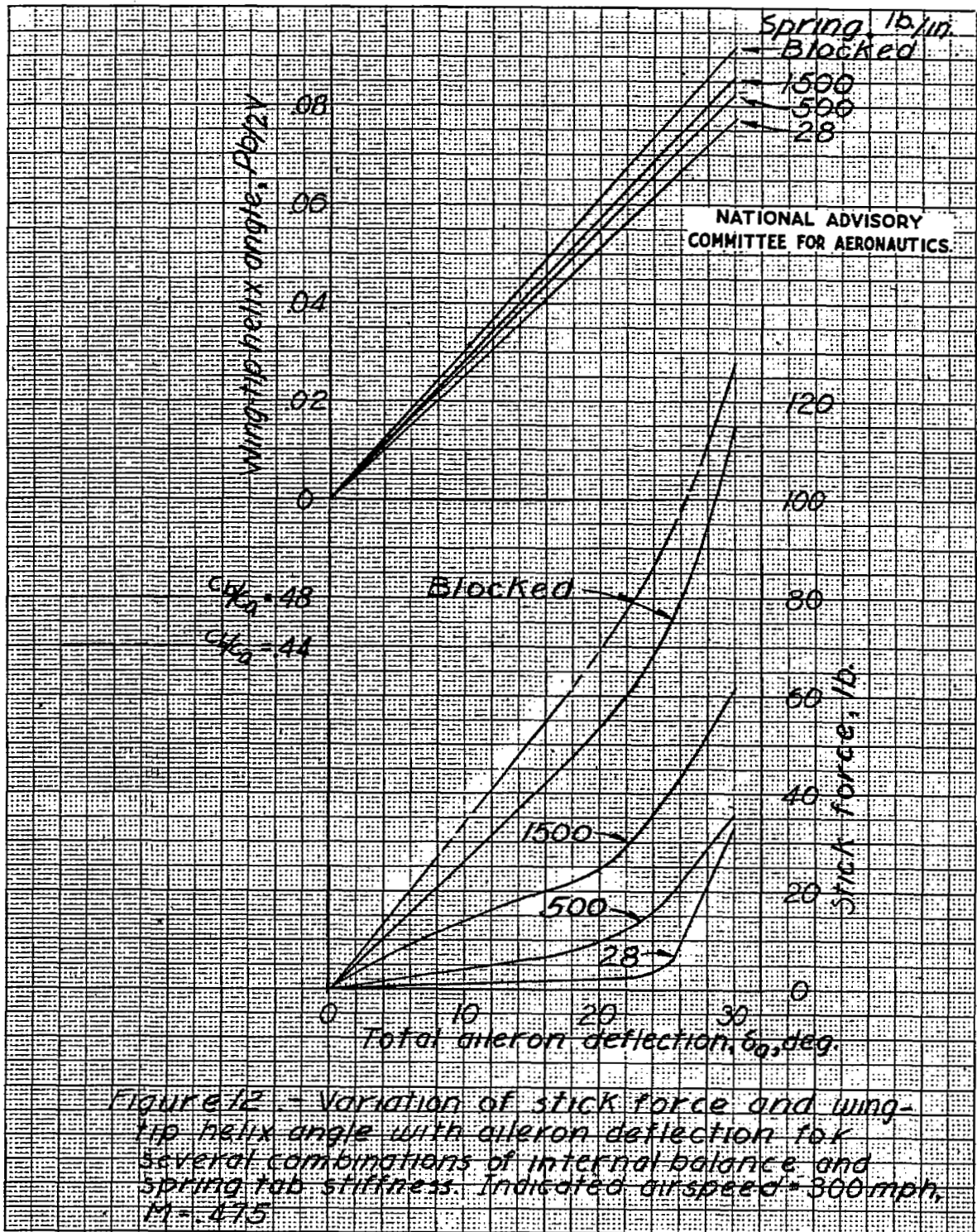
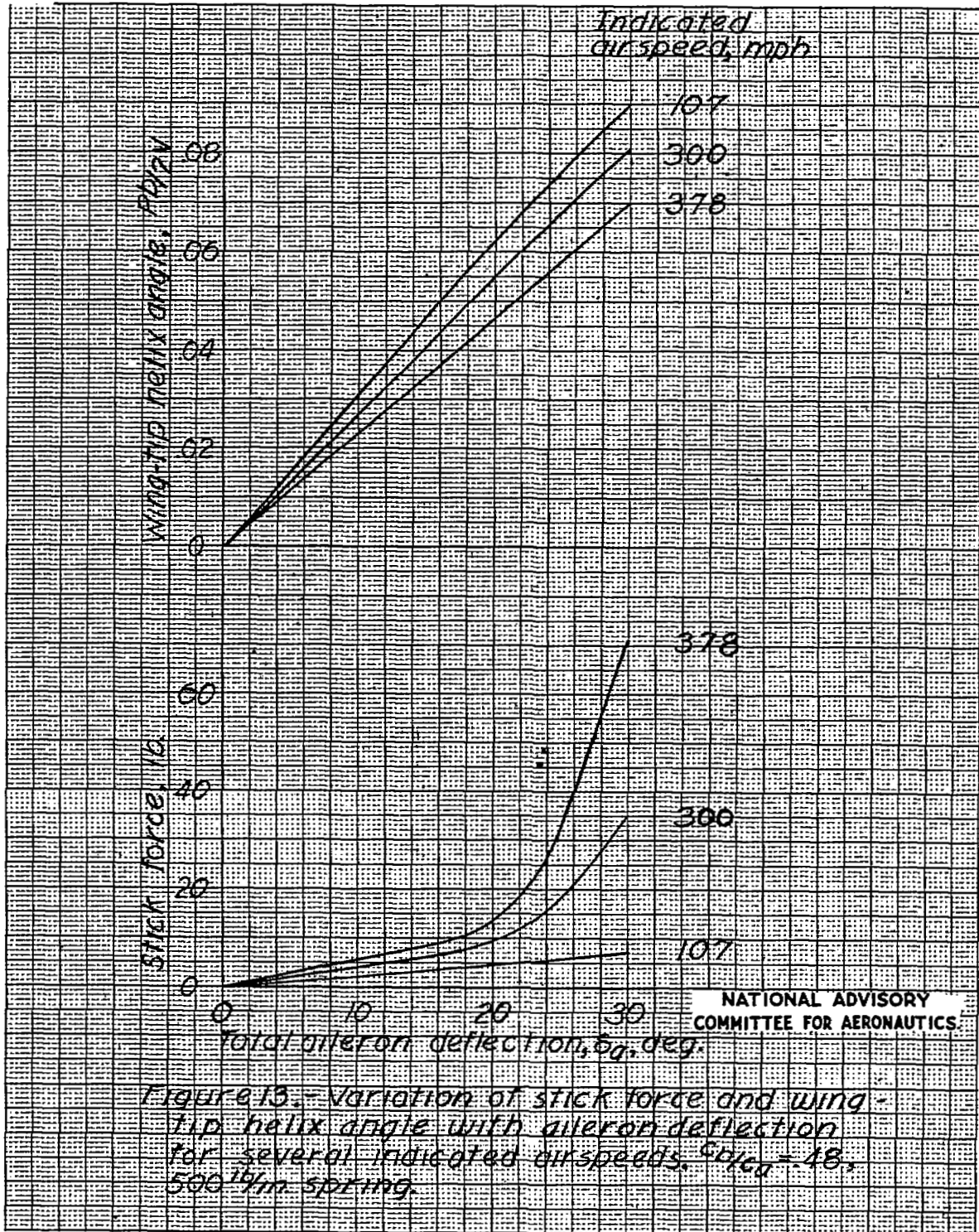
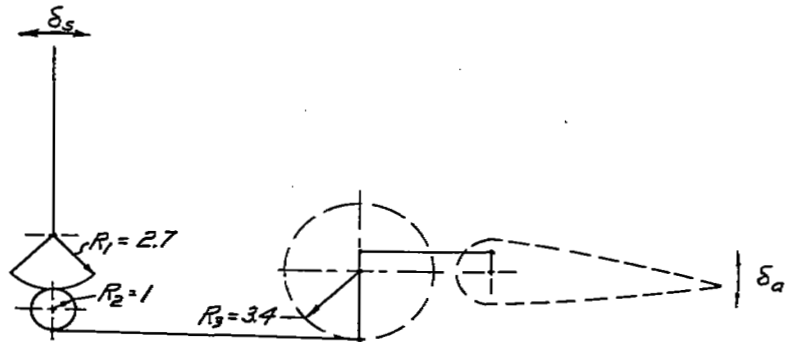


Figure 12 - Variation of stick force and wing-tip helix angle with aileron deflection for several combinations of internal balance and spring tab stiffness. Indicated airspeed = 300 mph, $M = 0.75$

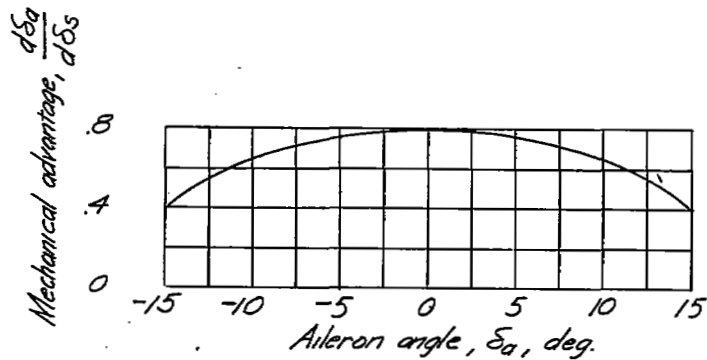


NATIONAL ADVISORY COMMITTEE FOR AERONAUTICS

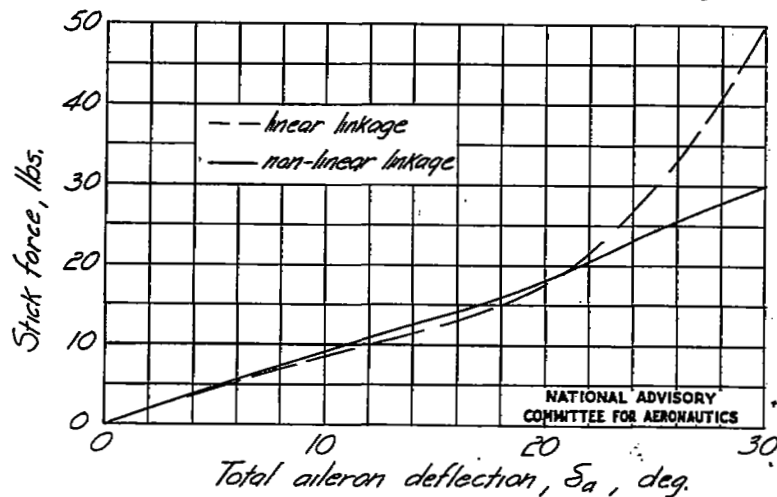
Figure 13.- Variation of stick force and wing-tip helix angle with aileron deflection for several indicated airspeeds. $C_{l_{\delta a}} = 18$, 500 lb/in spring.



a) Schematic sketch of assumed linkage

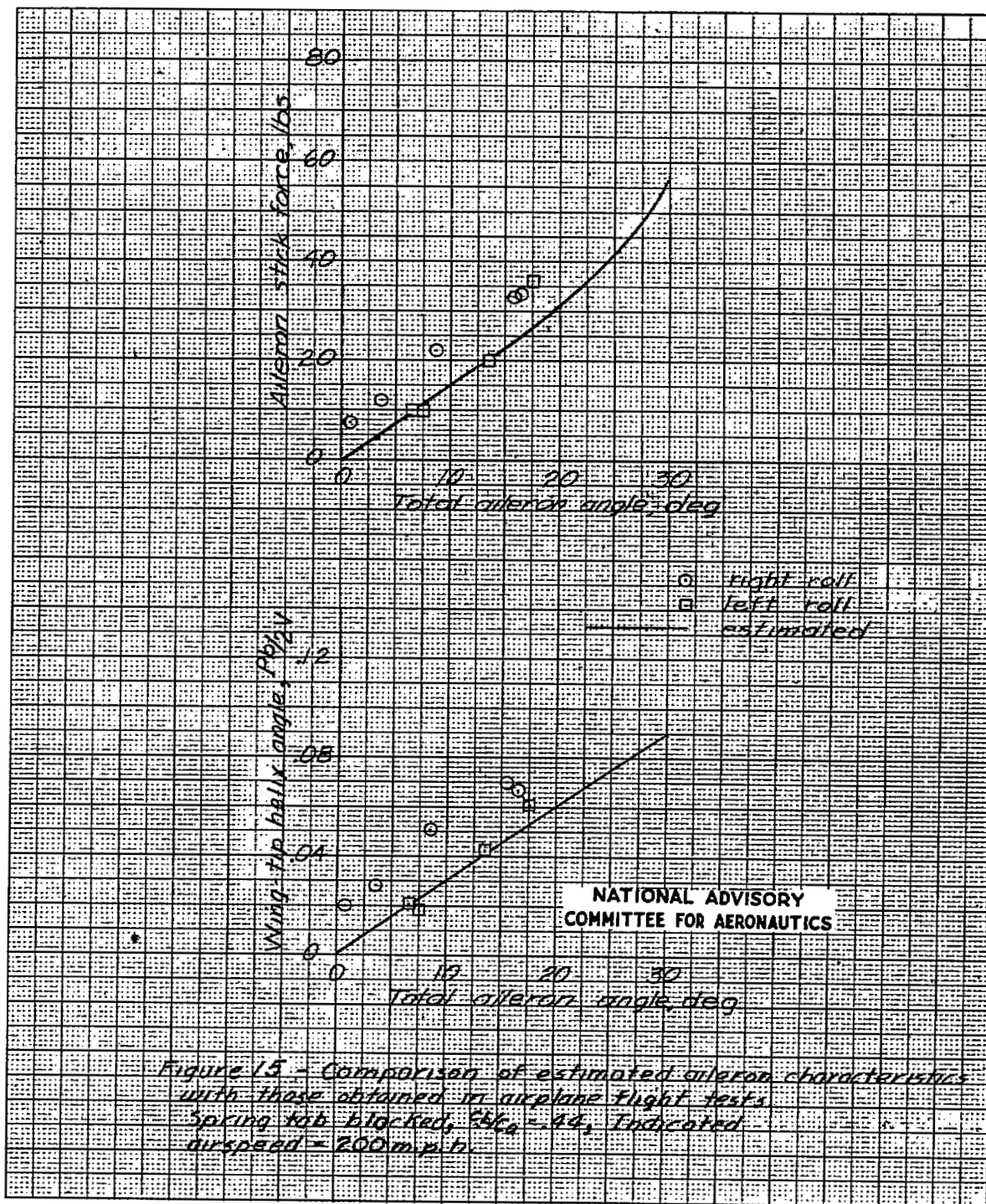


b) Variation of mechanical advantage with aileron deflection for assumed linkage



c) Estimated variation of stick force with aileron deflection for .48 $C_{L\alpha}$ internal balance, 1000 lb/in. spring, 300 m.p.h. indicated airspeed.

Figure 14.- Linkage and stick force characteristics for non-linear aileron-stick linkage.



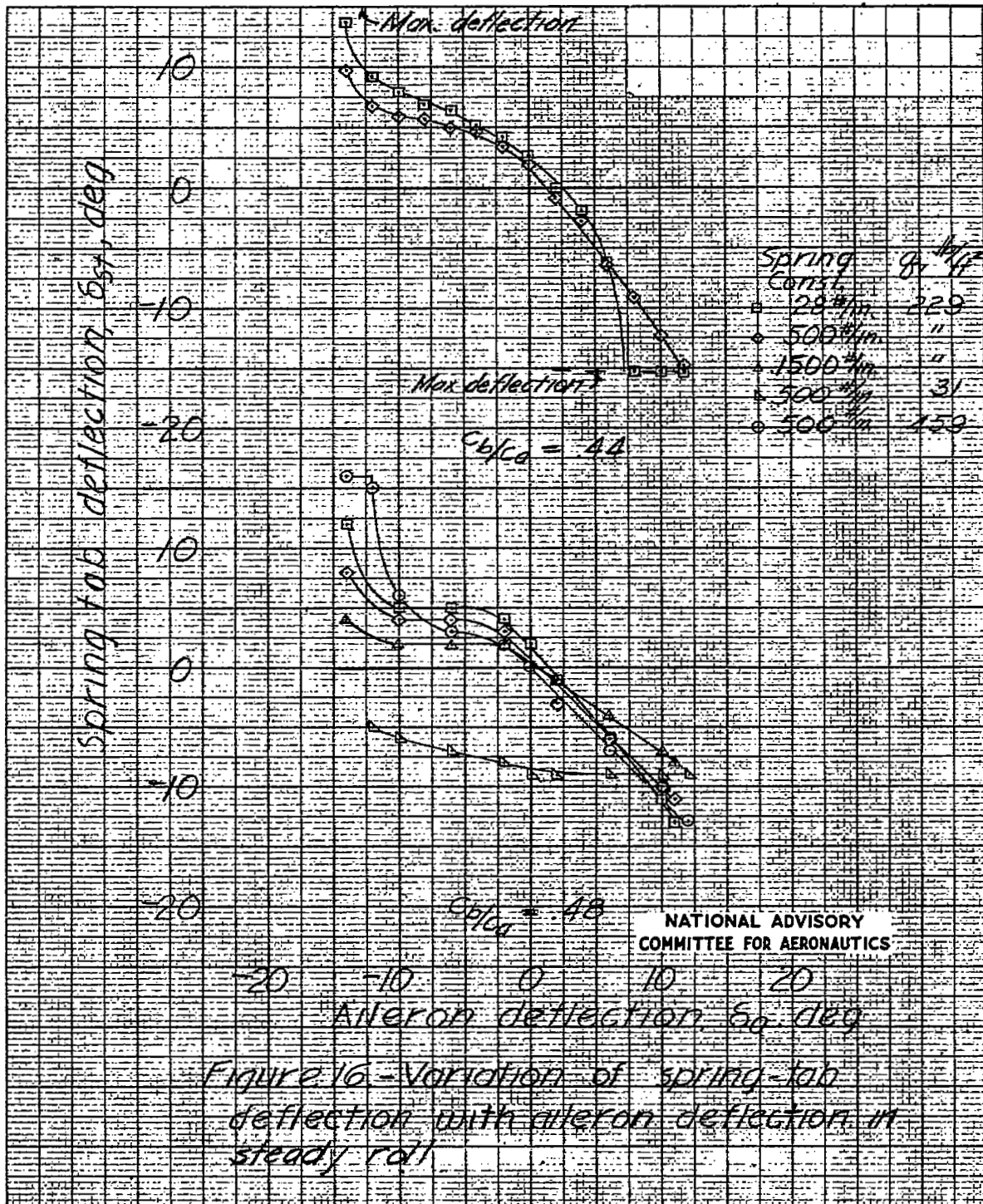


Figure 16 - Variation of spring-tab deflection with aileron deflection in steady roll

1957

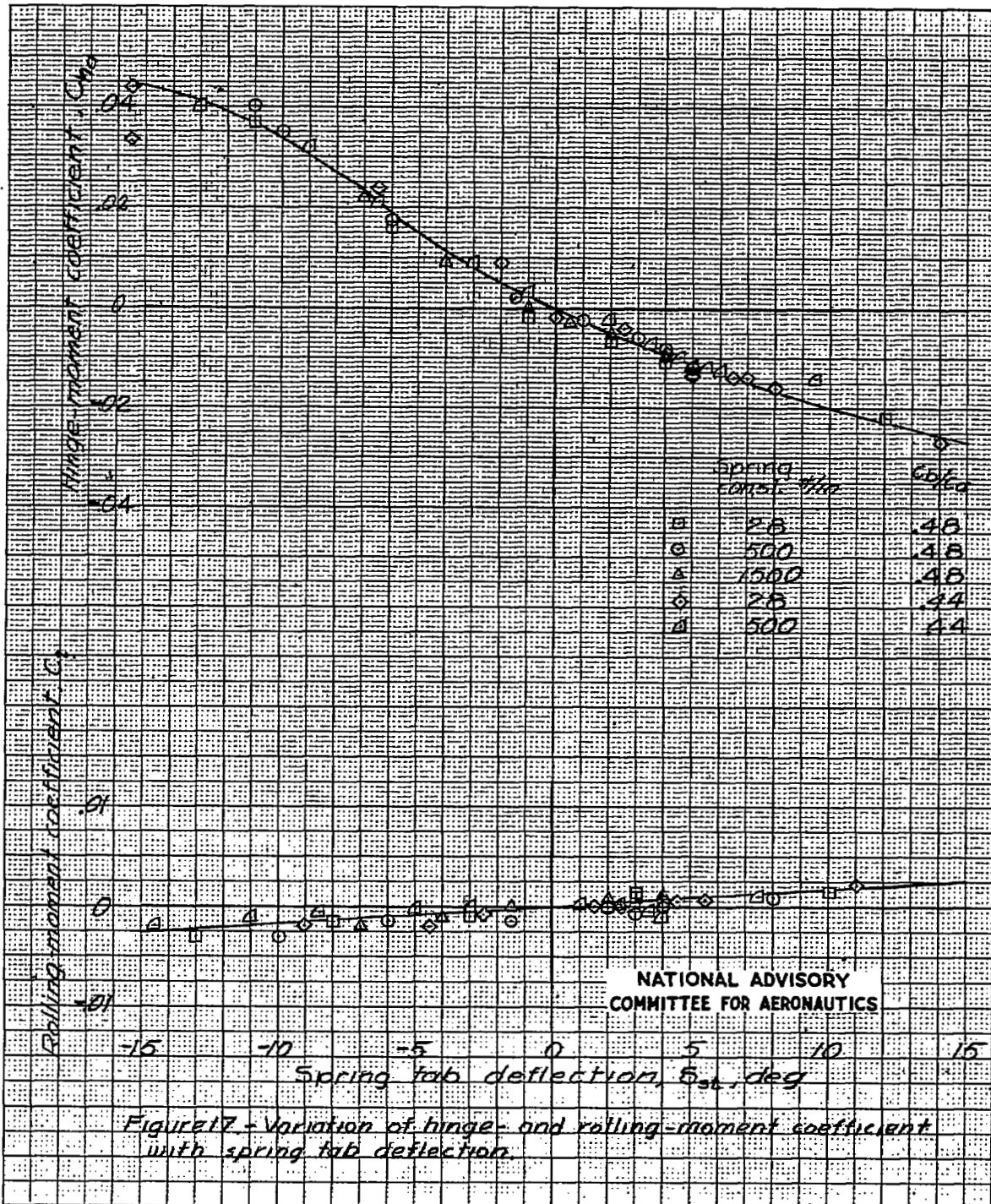
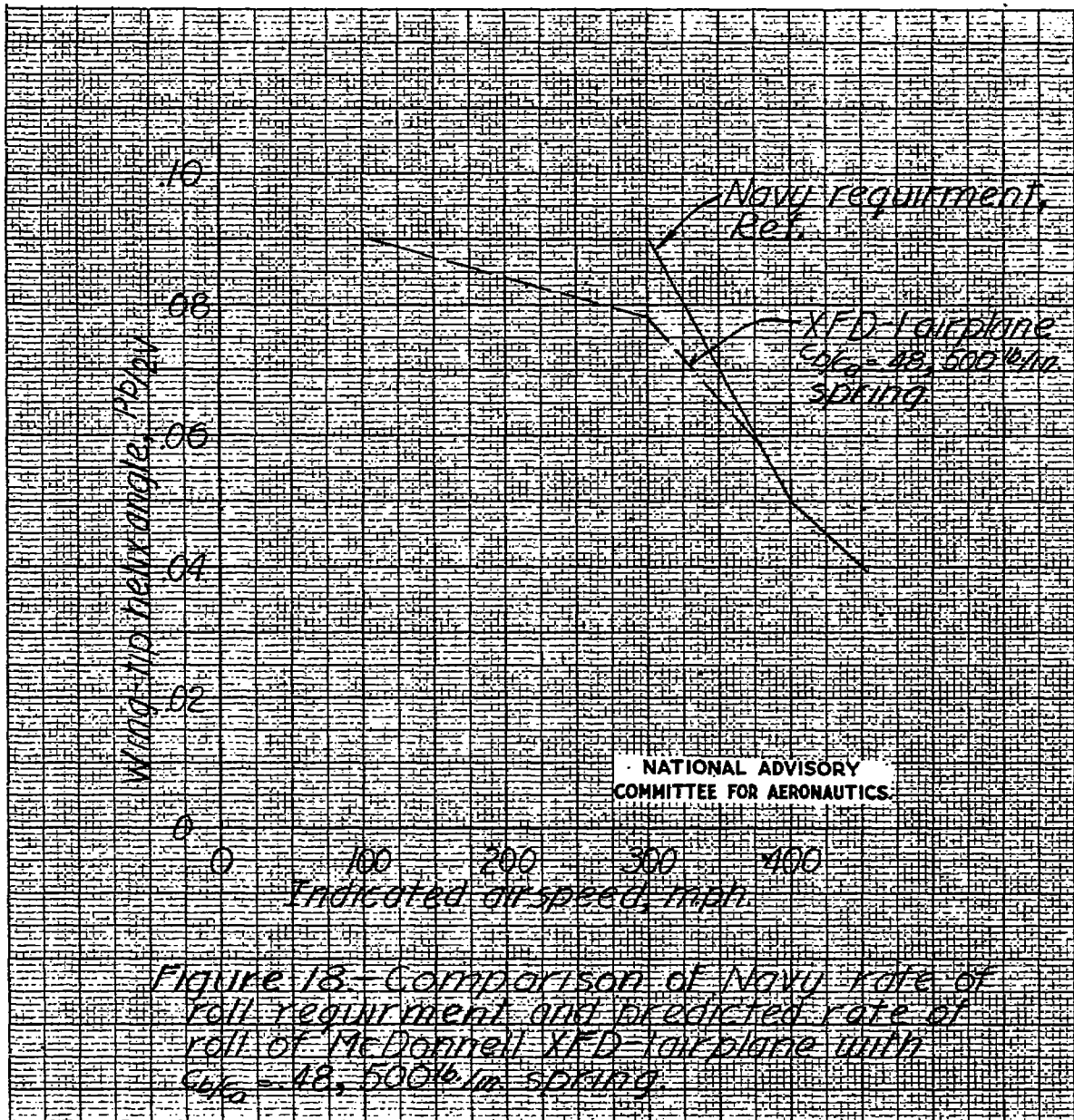


Figure 17 - Variation of hinge- and rolling-moment coefficient with spring tab deflection.

NATIONAL ADVISORY
COMMITTEE FOR AERONAUTICS



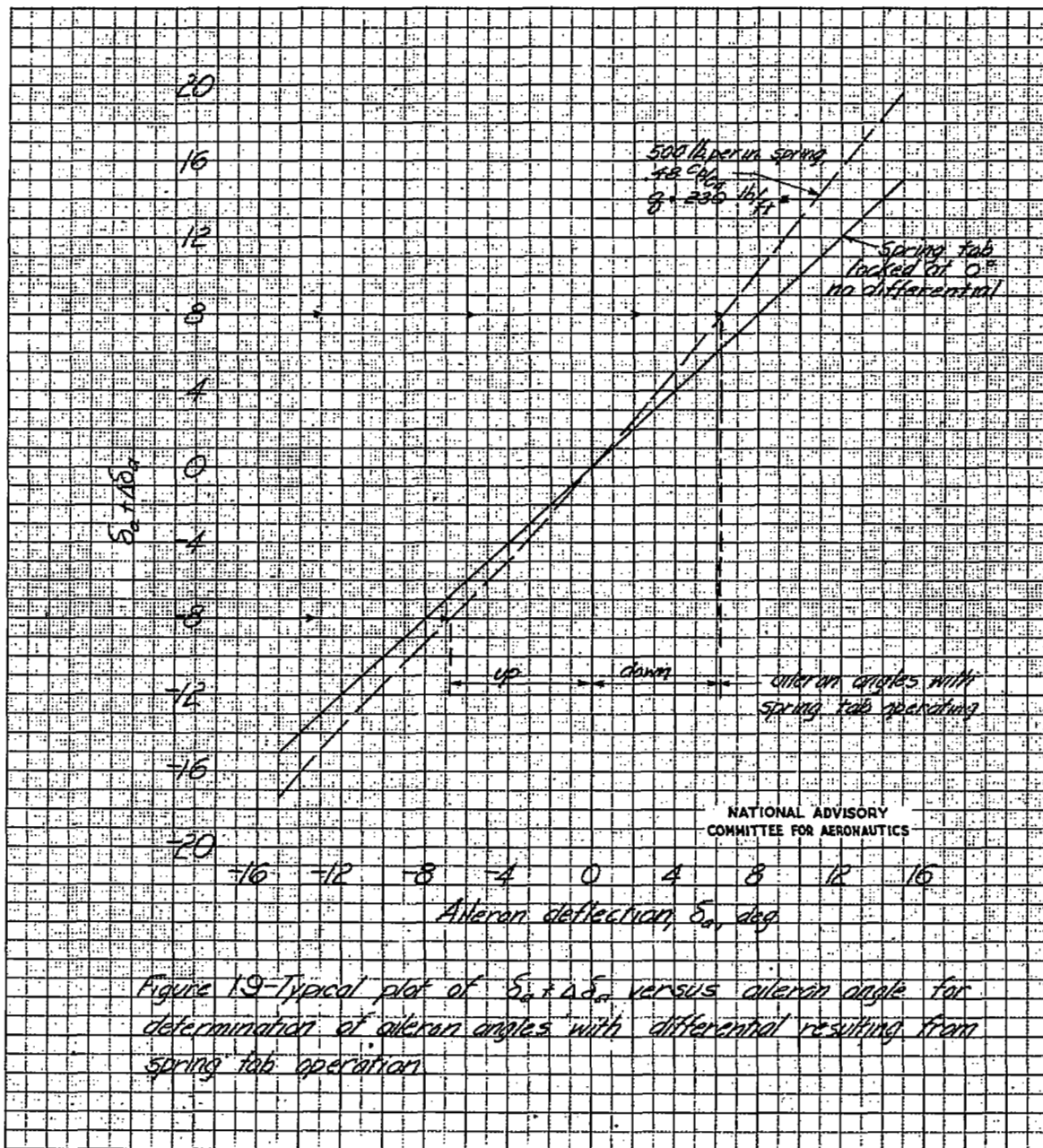


Figure 19—Typical plot of $\delta_s \pm \Delta \delta_a$ versus aileron angle for determination of aileron angles with differential resulting from spring tab operation.